Stem Cell Reports
Article

OPEN ACCESS

Lineage Reprogramming of Astroglial Cells from Different Origins into Distinct Neuronal Subtypes

Malek Chouchane,[1,3] Ana Raquel Melo de Farias,[1] Daniela Maria de Sousa Moura,[1] Markus Michael Hilscher,[1,4] Timm Schroeder,[2] Richardson Naves Leão,[1] and Marcos Romualdo Costa[1,*]

[1]Brain Institute, Federal University of Rio Grande do Norte, Natal 59056-450, Brazil
[2]Department of Biosystems Science and Engineering, ETH Zurich, Mattenstrasse 26, 4058 Basel, Switzerland
[3]Present address: Department of Neurological Surgery, University of California San Francisco, San Francisco, CA 94158, USA
[4]Present address: Institute for Analysis and Scientific Computing, Vienna University of Technology, 1040 Vienna, Austria
*Correspondence: mrcosta@neuro.ufrn.br
http://dx.doi.org/10.1016/j.stemcr.2017.05.009

SUMMARY

Astroglial cells isolated from the rodent postnatal cerebral cortex are particularly susceptible to lineage reprogramming into neurons. However, it remains unknown whether other astroglial populations retain the same potential. Likewise, little is known about the fate of induced neurons (iNs) in vivo. In this study we addressed these questions using two different astroglial populations isolated from the postnatal brain reprogrammed either with *Neurogenin-2* (*Neurog2*) or *Achaete scute homolog-1* (*Ascl1*). We show that cerebellum (CerebAstro) and cerebral cortex astroglia (CtxAstro) generates iNs with distinctive neurochemical and morphological properties. Both astroglial populations contribute iNs to the olfactory bulb following transplantation in the postnatal and adult mouse subventricular zone. However, only CtxAstro transfected with *Neurog2* differentiate into pyramidal-like iNs after transplantation in the postnatal cerebral cortex. Altogether, our data indicate that the origin of the astroglial population and transcription factors used for reprogramming, as well as the region of integration, affect the fate of iNs.

INTRODUCTION

Direct lineage reprogramming of somatic cells into induced neurons (iNs) is a promising strategy to study the molecular mechanisms of neuronal specification, identify potential therapeutic targets for neurological diseases, and eventually repair the CNS after acute or neurodegenerative injury (Arlotta and Berninger, 2014). Brain resident cells such as forebrain astrocytes present some great advantages when we consider the easiness and efficiency of conversion into iNs both in vitro (Berninger et al., 2007) and in vivo (Guo et al., 2014; Hu et al., 2015; Niu et al., 2013, 2015) compared with other cell types (Vierbuchen et al., 2010; Pang et al., 2011; Victor et al., 2014).

However, still little is known about the role of the environment in the specification of iNs fates during astroglia lineage reprogramming in vivo (Heinrich et al., 2015). Also, which are the subtypes of iNs generated by lineage reprogramming and how they could be controlled remain poorly understood. Following retroviral-mediated expression of ACHAETE SCUTE HOMOLOG-1 (ASCL1) or NEUROGENIN-2 (NEUROG2) in vitro, forebrain astrocytes are reprogrammed mostly into GABAergic or glutamatergic neurons, respectively (Heinrich et al., 2010). These observations led to the suggestion that ASCL1 and NEUROG2 would be instructing neuronal phenotypes, reminiscent of their reported role in cortical development (Schuurmans and Guillemot, 2002). However, the same transcription factors (TFs) are also expressed by non-overlapping progenitor populations in the developing cerebellum, contributing to the generation of GABAergic neurons in cerebellar nuclei, Purkinje cells, and inhibitory interneurons of the cerebellar cortex (Zordan et al., 2008). Thus, it is possible that astroglial cells isolated from cerebral cortex or cerebellum and lineage reprogrammed with NEUROG2 or ASCL1 could retain a "molecular memory" of their origin and generate iNs with distinctive phenotypes.

To test this possibility, we first investigated the potential to reprogram astroglial cells isolated from the postnatal cerebellum (CerebAstro) into iNs. Next, we compared the phenotypes of iNs derived from lineage-reprogrammed CerebAstro and cerebral cortex astroglia (CtxAstro), both in vitro and in vivo, following transplantation in the mouse cerebral cortex or subventricular zone (SVZ). Our results show that either ASCL1 or NEUROG2 is sufficient to convert CerebAstro into iNs adopting mostly a GABAergic phenotype. Following transplantation in the postnatal subventricular zone, both types of astroglial cells generate iNs that migrate to the olfactory bulb and integrate as granular or periglomerular neurons, albeit at different ratios depending on the reprogrammed astroglial population. However, after transplantation in the postnatal cerebral cortex, only iNs derived from CtxAstro reprogrammed with NEUROG2 adopted fates reminiscent of cortical pyramidal neurons. Collectively, our results suggest that both the origin of the astroglial population used for reprogramming and the region of grafting in the brain affect the phenotype of iNs.

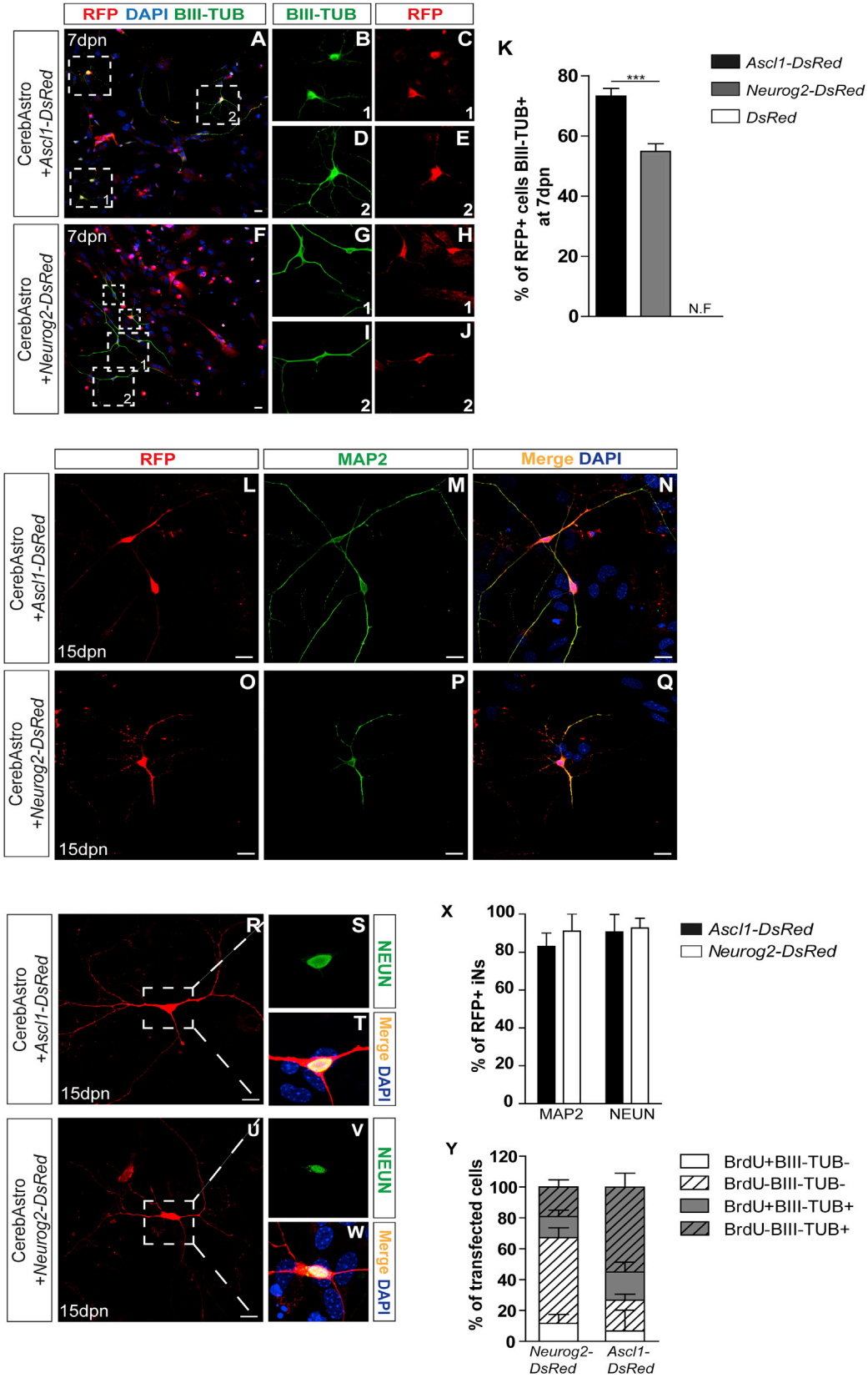

(legend on next page)

RESULTS

Expression of ASCL1 or NEUROG2 Efficiently Reprograms Cerebellum Astroglia in iNs

Direct lineage reprogramming of astroglial cells into iNs following viral or chemical delivery of neurogenic TFs is well established for astrocytes isolated from the cerebral cortex of postnatal mice (Berninger et al., 2007; Gascón et al., 2015; Heinrich et al., 2010; Masserdotti et al., 2015). However, it remains unknown whether astroglial cells from different regions of the CNS hold the same potential. To address this possibility, we set out to investigate whether the expression of single proneural TFs could lineage reprogram CerebAstro into iNs. Toward this aim, we generated cultures enriched for cerebellum astroglia and nucleofected the cells with plasmids carrying the genes encoding for NEUROG2 (*Neurog2-DsRed*), ASCL1 (*Ascl1-DsRed*), or only the reporter protein dsRed (*dsRed*). To determine the cellular composition of cultures prior to nucleofection, we immunostained cells for the astrocytic marker glial fibrillary acidic protein (GFAP), the pan-neuronal marker class III β-tubulin (BIII-TUBULIN), the neural stem cell transcription factor SOX2, and the oligodendrocyte marker O4. We observed that the vast majority of cells were positive for GFAP, whereas only a very small percentage of cells were positive for BIII-TUBULIN (GFAP: 93% ± 1%; BIII-TUBULIN: 3% ± 1%; n = 2,254 cells) (Figures S1A–S1E). We did not detect expression of O4 and SOX2 in the cultures (data not shown). One day post nucleofection (dpn), we observed that virtually all transduced cells expressed GFAP (Figures S1H–S1J). However, at 7–8 dpn most CerebAstro transduced with ASCL1 or NEUROG2 adopted a neuronal-like morphology and expressed BIII-TUBULIN (Figures 1A–1K; ASCL1: 73% ± 2% BIII-TUBULIN$^+$ cells, n = 1,320 dsRed $^+$ cells; NEUROG2: 54% ± 2% BIII-TUBULIN$^+$ cells, n = 1,234 dsRed $^+$ cells). In sharp contrast, cells nucleofected with dsRed kept astrocyte morphology and did not express BIII-TUBULIN (Figures S1F–S1G). Similar rates of iNs were observed with cerebral cortex astroglia nucleofected with *Neurog2-DsRed*, *Ascl1-DsRed*, or control plasmids (Figures S1K–S1Q), indicating that CerebAstro and CtxAstro are equally prone to lineage reprogramming into iNs after expression of NEUROG2 or ASCL1. According to previous data in the literature (Lawyell et al., 2000; Masserdotti et al., 2015), we also observed that the capacity of CerebAstro and CtxAstro to generate multipotent neurospheres and to lineage reprogramming decreased after successive passages in vitro (Figures S1R–S1U).

Next, we studied the process of CerebAstro lineage reprogramming into neuron using time-lapse video-microscopy (Figure S2 and Movies S1, S2, and S3). We observed that most transfected cells in control or experimental conditions displayed astroglial morphology. However, only cells transduced with either *Neurog2-DsRed* or *Ascl1-DsRed* underwent a thorough process of morphological changes ending with the acquisition of a neuronal-like morphology and the expression of neuron-specific markers (Figures S2A–S2L and Movies S1, S2, and S3). Yet expression of ASCL1 and NEUROG2 induced cell death in a high percentage of cells (Figure S2M), suggesting that, similar to cerebral cortex astroglia, the reprogramming process can be hampered by metabolic constraints (Gascón et al., 2015). Notably, we also observed that few transfected cells underwent cell division (Figure S2N), suggesting that mostly postmitotic astroglial cells are converted into iNs. Accordingly, most iNs were generated without cell division, as indicated by the low proportion of iNs incorporating bromodeoxyuridine (BrdU) after expression of NEUROG2 or ASCL1 (Figure 1Y). To further confirm the astroglial nature of lineage-converted cells, we genetically labeled astrocytes using the double-transgenic GLAST-CreERT/CAG-CAT-GFP mouse (Heinrich et al., 2010). Animals received tamoxifen through the mother milk from postnatal day 5 (P5) to P7, leading to the Cre-mediated recombination in cerebellum astroglia in vivo (Figure S3A). We observed that 95% of iNs also expressed GFP, confirming the astroglial origin of the original cells.

Figure 1. ASCL1 and NEUROG2 Convert Cerebellum Astroglia into Induced Neurons

(A–J) Representative pictures taken from CerebAstro cultures 7 days post nucleofection (dpn) with *Ascl1-DsRed* (A) or *Neurog2-DsRed* plasmid (F). Many nucleofected RFP$^+$ cells (inside dotted boxes) adopt neuronal-like morphologies and express the immature neuronal marker BIII-TUBULIN (BIII-TUB) after transduction with (A) ASCL1, magnification of boxes 1 and 2 in (B) to (E) or (B) NEUROG2, magnification of boxes 1 and 2 in (G) to (J).

(K) Quantification of BIII-TUB expression in CerebAstro culture 7 dpn with *Ascl1-DsRed* (black bar), *Neurog2-DsRed* (gray bar), or control plasmid *dsRed* (white bar) (see Figure S1 for control condition). ***p < 0.001. N.F, not found.

(L–W) Expression of mature neuronal markers in lineage-reprogrammed CerebAstro iNs 15 dpn. Example of RFP$^+$ ASCL1-iNs (L–N) and NEUROG2-iNs (O–Q), stained for MAP2. Example of RFP$^+$ ASCL1-iNs (R–T) and NEUROG2-iNs (U–W) stained for NEUN.

(X) Quantification of MAP2$^+$ and NEUN$^+$ among RFP$^+$ cells 15dpn with ASCL1 (black bar) or NEUROG2 (white bar).

(Y) Quantification of BrdU incorporation and BIII-TUB expression in nucleofected cells 8 dpn with ASCL1 or NEUROG2. Nuclei are stained with DAPI (blue).

Data are derived from six independent experiments (mean ± SEM). Scale bars, 25 μm. See Figures S1–S3.

Functional Properties of Cerebellum Astroglia-Derived iNs

After, we investigated the phenotypic maturation of lineage-reprogrammed CerebAstro iNs. For this, nucleofected cultures were maintained for 2 weeks in differentiation medium and assessed for the expression of the neuronal microtubule-associated protein 2 (MAP2) and the neuronal nuclei protein Foxb3 (NEUN). We observed that CerebAstro transfected with either ASCL1 or NEUROG2 reprogrammed into iNs expressing MAP2 (ASCL1: 83% ± 7%, n = 321 cells; NEUROG2: 91% ± 9%, n = 236 cells) and NEUN (ASCL1: 90% ± 9%, n = 365 cells; NEUROG2: 92% ± 5%, n = 210 cells) (Figures 1L–1X). To further stimulate the synaptic maturation of iNs, we grew transfected CerebAstro in the presence of co-cultured neurons (see Supplemental Experimental Procedures). Thirty days after nucleofection we could observe expression of SYNAPSIN 1, a synaptic vesicle protein involved in the control of neurotransmitter release (Hvalby et al., 2006), in juxtaposition to dsRed$^+$ processes (Figures 2A–2H), suggesting that iNs could be establishing synaptic contacts with co-cultured neurons.

To study the electrical properties of iNs, we performed patch-clamp recordings of fourteen ASCL1-iNs and nine NEUROG2-iNs grown in the absence of co-cultured primary neurons (Figures 2I–2L). Of the 14 ASCL1-iNs, ten responded with action potentials and had a mean input resistance of 337 ± 76 MΩ, a mean resting membrane potential of −52 ± 2 mV, and a mean action potential amplitude of 50 ± 7 mV following minimal depolarizing current injections (50 pA, 500 ms) (Figure 2L). NEUROG2-iNs (n = 9 cells) had a mean input resistance of 352 ± 78 MΩ, a mean resting membrane potential of −56 ± 2 mV, and a mean action potential amplitude of 42 ± 4 mV following the same current injection (50 pA, 500 ms) (Figure 2L). Hyperpolarizing currents (−100 pA, 500 ms) generated rebound action potentials in 50% (5/10) of the *ASCL1*-cells with a mean amplitude of 63 ± 4 mV and 22% (2/9) of the NEUROG2-cells with a mean amplitude of 39 ± 2 mV (Figure 2I). Notably, some iNs showed spontaneous electrical activity, further suggesting that iNs established synaptic contacts in the culture (Figure 2I). Recorded iNs could be classified into cells with spikelets (40% of ASCL1-iNs; 66% of NEUROG2-iNs), cells with a few spikes (40% of ASCL1-iNs; 22% of NEUROG2-iNs), and regular spiking cells (30% of ASCL1-iNs; 11% of NEUROG2-iNs) (Figures 2I and 2J). Moreover, current-voltage relationships of ASCL1-iNs and NEUROG2-iNs revealed a significant difference between instantaneous values in response to hyperpolarizing current injections (Figure 2K). Collectively, these observations suggest that NEUROG2 or ASCL1 can efficiently reprogram cerebellum astroglia into functional iNs.

ASCL1 and NEUROG2 Induce Different Neuronal Subtypes in Astroglia of Different Origin

Another important aspect of neuronal differentiation is the establishment of axial polarity and process growth (Barnes and Polleux, 2009; Whitford et al., 2002; Takano et al., 2015). Interestingly, we noted that iNs displayed different morphologies 15 days after expression of ASCL1 or NEUROG2 in CerebAstro or CtxAstro (Figure S4). To quantify these differences, we analyzed morphological features of iNs using the Sholl analysis. We found that iNs derived from CerebAstro expressing ASCL1 displayed significantly longer processes, with an increased amount of secondary and tertiary branches compared with iNs expressing NEUROG2 (Figure S4F). Notably, we also found that iNs derived from CerebAstro expressing ASCL1 were more complex than those derived from CtxAstro expressing the same TF, whereas the opposite was observed with NEUROG2 (Figures S4H–S4I).

Next, we set out to measure the axial distribution of cell processes (Figures S4G and S4K). We observed that expression of ASCL1 in CerebAstro generate higher polarized iNs than NEUROG2 (Figure S4G). The opposite result was observed when we compared iNs derived from CtxAstro (Figure S4K). Collectively, these morphological parameters indicate that both the TF and the type of reprogrammed astroglial cell may interfere with iNs phenotypes.

To further investigate possible phenotypic distinctiveness of iNs, we analyzed the expression of the neurotransmitter GABA and glutamate, as well as TBR1, a TF associated with glutamatergic neurons (Hevner et al., 2006), in iNs derived from CerebAstro or CtxAstro (Figures 3 and S5). We observed that the percentage of GABA was higher than GLUTAMATE-expressing iNs following expression of both ASCL1 and NEUROG2 in CerebAstro (Figures 3A–3S; CerebAstro GABA$^+$ iNs ASCL1: 70% ± 6%, n = 68 cells and NEUROG2: 59% ± 7%, n = 58 cells; CerebAstro Glut$^+$ iNs ASCL1: 38% ± 6%, n = 52 cells and NEUROG2: 48% ± 2%, n = 63). The GABAergic phenotype of astroglia-derived iNs was also confirmed using astrocytes isolated from GAD67-GFP mice (Figures 3T–3Z′). In contrast, the same TFs induced different fates in CtxAstro. While iNs derived from CtxAstro reprogrammed with NEUROG2 expressed mostly GLUTAMATE, ASCL1 induced more GABA expression (Figures 3S and S5G–S5L; CtxAstro GABA$^+$ iNs ASCL1: 64% ± 15%, n = 60 cells and NEUROG2: 19% ± 7%, n = 50 cells; CtxAstro GLUT$^+$ iNs ASCL1: 50% ± 9%, n = 67cells and NEUROG2: 81% ± 4%, n = 54 cells). We also noted that NEUROG2 induced the expression of TBR1 only in CtxAstro (Figures S5A–S5F; 79% ± 2% of TBR1$^+$, n = 30 iNs).

Next, to evaluate whether iNs derived from CtxAstro or CerebAstro adopt the phenotype of distinct GABAergic classes, we compared the expression of the calcium binding

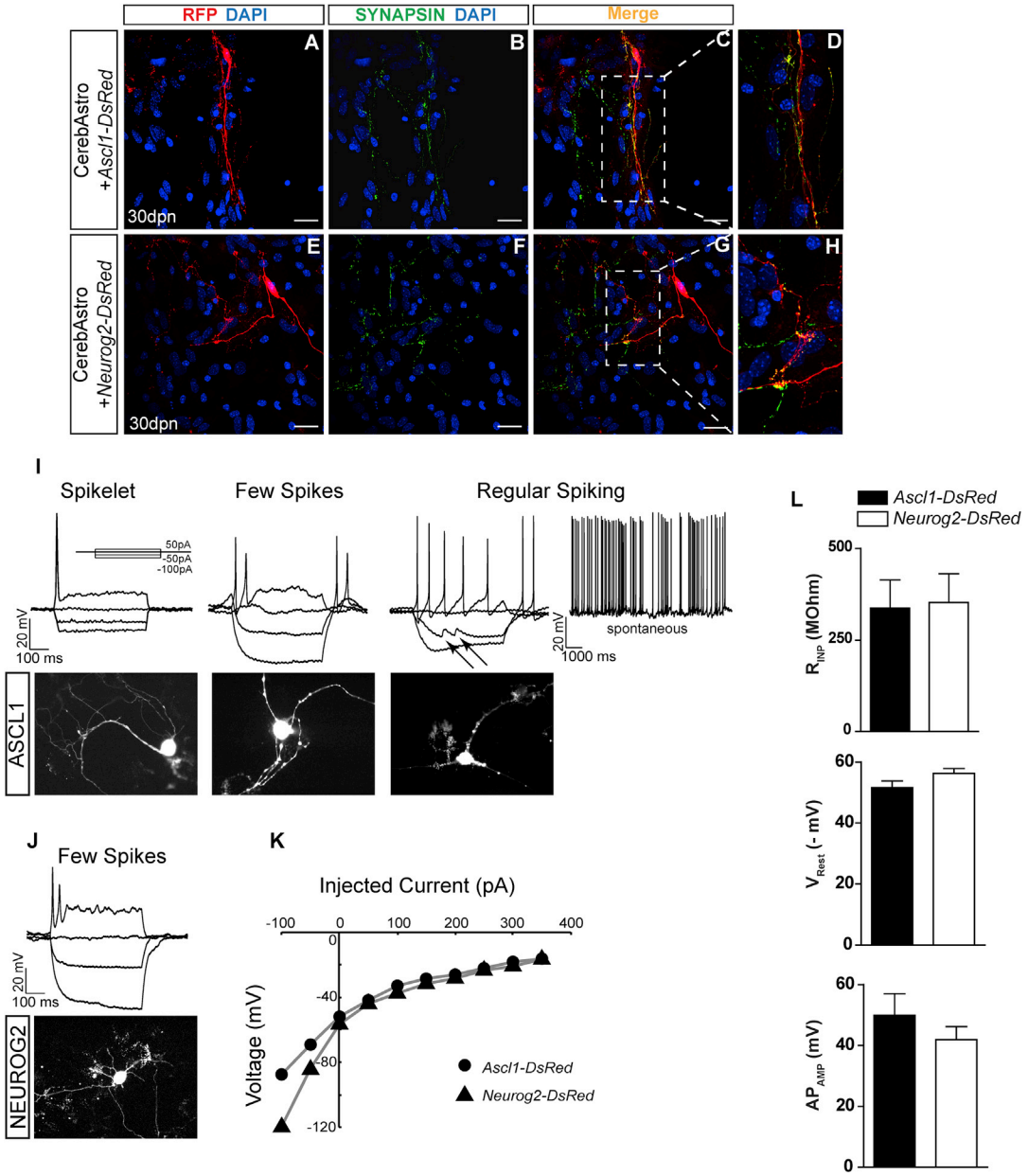

Figure 2. Electrical and Synaptic Development of CerebAstro-Derived iNs

(A–H) Lineage-reprogrammed CerebAstro iNs express SYNAPSIN 1 (green) 30 dpn with *Ascl-DsRed* or *Neurog2-DsRed* plasmids. Example of RFP$^+$/SYNAPSIN$^+$ iNs 30 dpn with ASCL1 (A–D) or NEUROG2 (E–H). (D–H) Magnifications of dashed boxes in (C) and (G), respectively.

(I–L) Electrophysiological properties of ASCL1- and NEUROG2-iNs. Current clamp traces from ASCL1-iNs showing spikelet (left), few spikes (middle), and regular spiking (right) in response to depolarizing current injections (50 pA, 500 ms) (I, top). Arrows highlight spontaneous excitatory postsynaptic potentials in recorded cells (I). Fluorescence images of the recorded ASCL1-iNs (I, bottom).

(J) Example of current clamp traces from a NEUROG2-iNs responding with a few spikes to depolarizing current injections (50 pA, 500 ms) (J, top). Note the deeper sag due to hyperpolarizing current injections (−100 pA, 500 ms) compared with ASCL1-iNs. Fluorescence image of the recorded NEUROG2-iN (J, bottom).

(K) Current-voltage relationships for ASCL1-iNs (circles) and NEUROG2-iNs (triangles) measured at the beginning of the onset of the current steps.

(L) Plot of mean input resistance, resting membrane voltage, and mean action potential amplitude following the current injection (50 pA, 500 ms) of ASCL1-iNs (black plot) and NEUROG2-iNs (white plot).

Data are derived from three independent experiments (mean ± SEM). Scale bars, 50 μm.

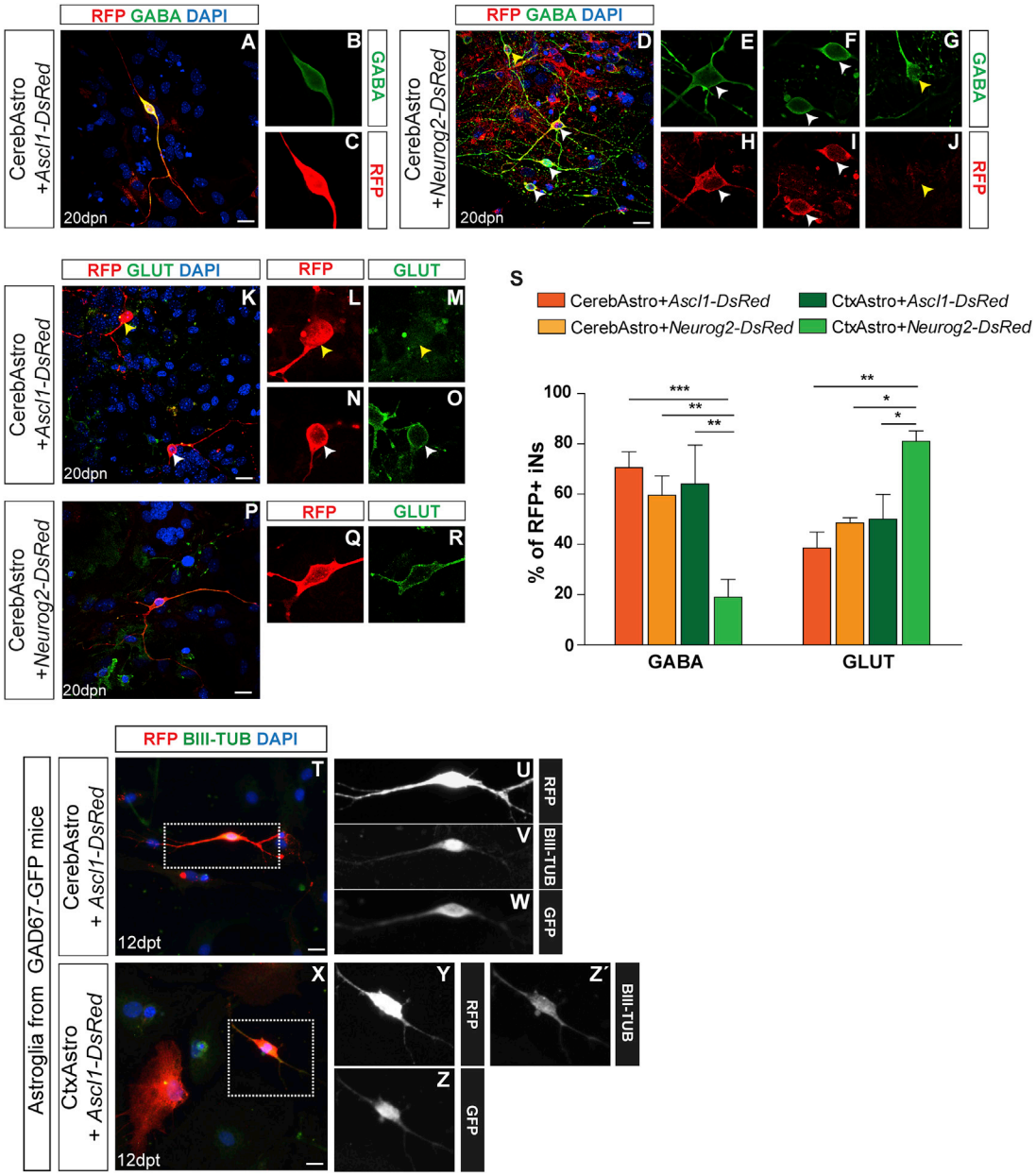

Figure 3. Lineage-Reprogrammed Cortical and Cerebellar iNs Adopt Different Neurotransmitter Phenotypes

(A–J) Examples of CerebAstro-derived RFP$^+$ iNs expressing GABA 20 dpn with either ASCL1 (A) or NEUROG2 (D). Single confocal z stacks are shown in higher magnification to confirm the colocalization of GABA and RFP in iNs (B, C, and E–J). Observe the similar pattern of GABA expression between co-cultured hippocampal neurons (RFP$^-$, yellow arrowhead in D) and iNs (RFP$^+$, white arrowheads in D).

(K–R) Example of CerebAstro-derived RFP$^+$ iNs expressing GLUT 20 dpn with either ASCL1 (K–O) or NEUROG2 (P–R). Single confocal z stacks are shown in higher magnification to confirm the colocalization of glutamate and RFP in iNs (B, C, and E–J). Observe the presence of GLUT$^-$ (K–M, yellow arrowhead) and GLUT$^+$ (K, N, and O, white arrowhead) RFP$^+$ iNs.

(S) Quantification of GABA$^+$ and GLUT$^+$ cells among RFP$^+$ iNs derived from CerebAstro nucleofected with ASCL1 (orange) or NEUROG2 (yellow) and CtxAstro nucleofected with ASCL1 (dark green) or NEUROG2 (light green). *$p < 0.05$, **$p < 0.01$, ***$p < 0.001$.

(T–Z′) Expression of GFP in CerebAstro and CtxAstro derived from GAD67-GFP mice 12 dpn with ASCL1. Example of RFP$^+$/GFP$^+$/BIII-TUB$^+$ iN derived from CerebAstro (T, dashed box magnified and showing single channels in U–W) or CtxAstro (X, dashed box magnified and showing single channels in Y–Z′). GLUT, GLUTAMATE; BIII-TUB, BIII-TUBULIN. Statistical test: two-way ANOVA followed by Bonferroni's post hoc test (mean ± SEM).

Data are derived from 3 independent experiments. Scale bars, 25 μm. See also Figure S5.

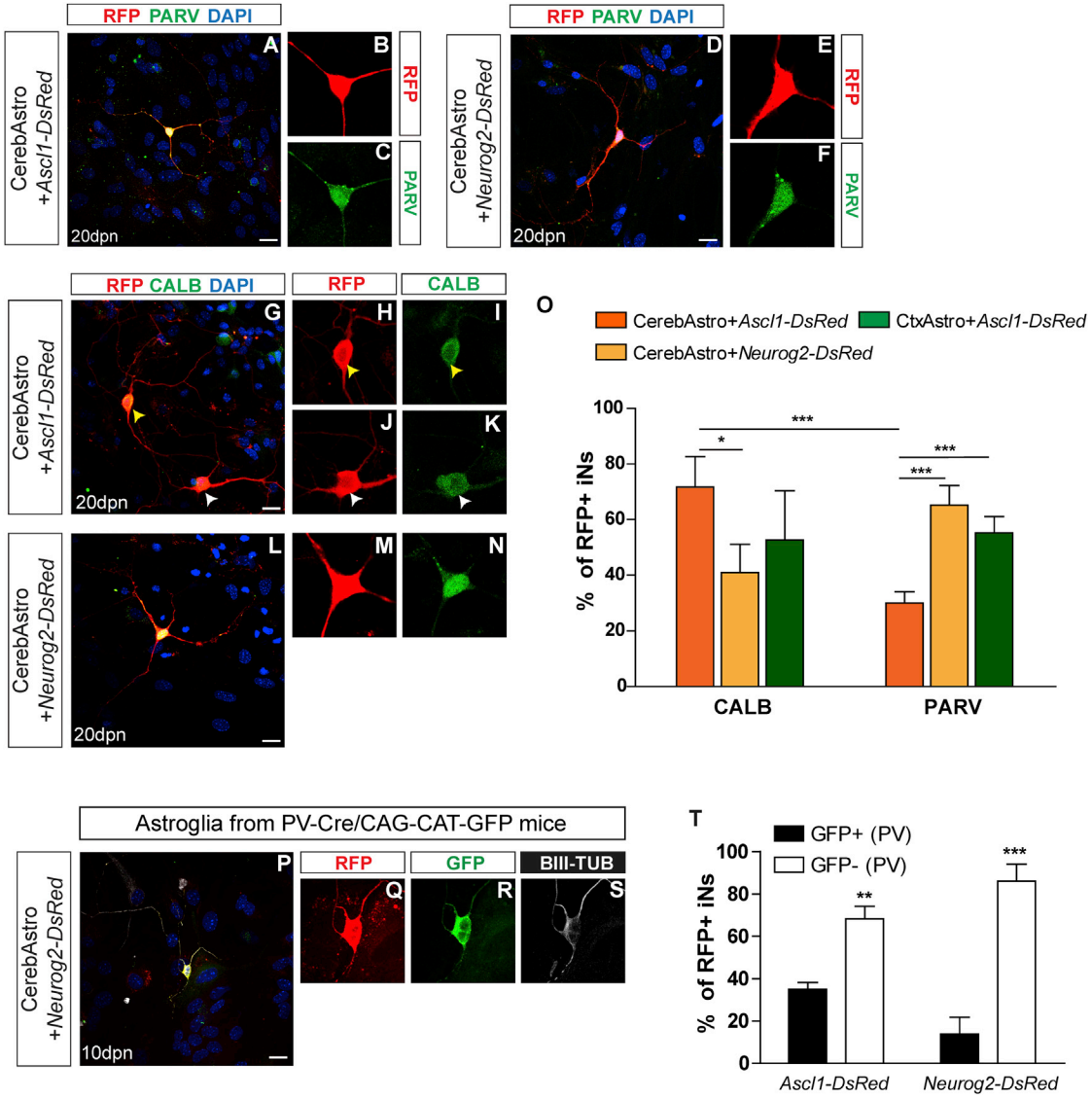

Figure 4. Expression of Calcium Binding Proteins Indicates that iNs Derived from Cortical and Cerebellar Astroglia Adopt Distinct GABAergic Phenotypes

(A–N) Examples of CerebAstro-derived iNs expressing PARV or CALB 30 dpn with either ASCL1 (A and G) or NEUROG2 (D and L). Single confocal z stacks of the two iNs (white and yellow arrowheads) are shown in higher magnification to confirm the colocalization of RFP with PARV (B, C, E, and F) or CALB (H–K, M, and N).

(O) Quantification of CALB$^+$ and PARV$^+$ cells among RFP$^+$ iNs derived from both CerebAstro nucleofected with either ASCL1 (orange) or NEUROG2 (yellow) and CtxAstro nucleofected with ASCL1 (green). *p < 0.05, ***p < 0.001.

(P) Example of NEUROG2-iN reprogrammed from CerebAstro isolated from PARV-Cre/CAG-CAT-GFP mice.

(Q–S) Single confocal z stacks are shown in higher magnification to confirm the colocalization of RFP, GFP, and BIII-TUB.

(T) Quantification of ASCL1-iNs and NEUROG2-iNs expressing GFP after lineage reprogramming of PARV-Cre/CAG-CAT-GFP CerebAstro (two-way ANOVA followed by Bonferroni's post hoc test, mean ± SEM). CALB, CALBINDIN; PARV, PARVALBUMIN; TUB, TUBULIN. **p < 0.01, ***p < 0.001.

Data are derived from three independent experiments. Scale bars, 20 μm. See also Figure S6.

proteins CALBINDIN (CALB) and PARVALBUMIN (PARV) in iNs after expression of NEUROG2 or ASCL1 (Figure 4). We observed that ASCL1 expression in CerebAstro induced a higher ratio of CALB$^+$ iNs, whereas NEUROG2 induced a higher ratio of PARV$^+$ iNs (Figures 4A–4O; ASCL1: 72% ± 11%, and NEUROG2 40% ± 10% CALB$^+$ iNs; n = 170 and

118 cells, respectively; ASCL1: 30% ± 4% and NEUROG2 65% ± 7% PARV$^+$ iNs; n = 120 and 143 cells, respectively). Interestingly, we also observed that more than half of CerebAstro-derived CALB$^+$ iNs expressed CTIP2 (Figure S6) a transcription factor present in Purkinje neurons (Leid et al., 2004). Additionally the parvalbuminergic phenotype of iNs was assessed using astrocytes isolated from PARV-Cre/CAG-CAT-GFP mice (Figures 3P–3T). We observed that 10 dpn with ASCL1 a similar proportion of iNs expressed GFP compared with iNs expressing PARV at 20 dpn (Figures 4O and 4T). However, the proportion of GFP$^+$ iNs at 10 dpn after NEUROG2 expression was lower than that expressing PARV at 20 dpn (Figures 4O and 4T), suggesting that the expression of PARV in NEUROG2-iNs is regulated at some point between 10 and 20 dpn.

In contrast, ASCL1 expression in CtxAstro induced similar rates of CALB$^+$ and PARV$^+$ iNs (Figure 4O; CALB: 53% ± 17% iNs; PARV: 55% ± 6% iNs; n = 138 and 127 cells, respectively). Yet ASCL1 induced a significantly higher fraction of PARV$^+$ iNs in CtxAstro compared with CerebAstro (Figure 4O). Altogether, these results indicate that ASCL1 and NEUROG2 instruct different subtypes of GABAergic iNs depending on the origin of the reprogrammed astroglial cell.

CtxAstro, but Not CerebAstro, Nucleofected with NEUROG2 Differentiate into Pyramidal-like Neurons after Transplantation in the Postnatal Mouse Cerebral Cortex

The distinctive iNs phenotypes observed in vitro raised the question as to whether these cells would keep such hallmarks after integration in a pre-existing circuitry. To investigate this possibility, we transplanted cortical and cerebellum astroglia following nucleofection with NEUROG2, ASCL1, or control plasmid in the postnatal mouse cerebral cortex and studied the phenotypes of grafted cells. To facilitate the identification of grafted cells, we transplanted astroglial cells isolated from GFP mice (Okabe et al., 1997) into wild-type animals. Twenty days post transplantation (dpt), animals were perfused and grafted cells were analyzed for their morphology and chemical markers (Figure 5). We observed that virtually all CtxAstro population nucleofected with control plasmid kept astroglial morphologies (Figures 5A and 5C; n = 1,145 GFP$^+$ cells, n = 4 host animals). Interestingly, astroglial cells adopted morphologies similar to those of endogenous astrocytes in the gray and white matter (Figures S7A–S7C; Emsley and Macklis, 2006). In sharp contrast, about one-fifth of CtxAstro nucleofected with NEUROG2 and transplanted into the postnatal cerebral cortex adopted neuronal morphologies in all animals analyzed (n = 2,338 GFP$^+$ cells in five host animals, 18% ± 7%) (Figures 5B–5O). Intriguingly, we noted that about half of iNs settled in the layers II/III of the cerebral cortex (Figure 5D). Induced neurons adopted a pyramidal neuron-like morphology with apical dendrites toward the molecular layer and basal dendrites projecting radially (Figures 5E and 5F). We also observed basal axonal processes directed toward the white matter (Figure 5E). Interestingly, some GFP$^+$ processes were observed in the contralateral corpus callosum (Figures S7K–S7O), suggesting that such processes originated from transplanted iNs. Some iNs showed very complex morphologies with several secondary and tertiary dendrites (Figure 5G), and the majority of these cells also showed dendritic spines (Figure 5I, 66% ± 8% of pyramidal-like iNs, n = 29 cells). Most cells with neuronal morphology also expressed NEUN$^+$ (Figures 5J–5L) and about 60% of iNs in layer II/III expressed the TF CUX1 (Figures 5M–5O, n = 15 cells). These data suggest that cortical astroglia reprogrammed with NEUROG2 can differentiate into pyramidal-like iNs in vivo.

In contrast, however, we found only a very small number of GFP$^+$ cells with neuronal morphology following transplantation of CerebAstro nucleofected with NEUROG2, as well as CtxAstro or CerebAstro nucleofected with ASCL1 (Figures S7D–S7I; >500 cells counted/animal). Still, different from iNs derived from CtxAstro reprogrammed with NEUROG2, those iNs displayed morphologies reminiscent of non-spiny GABAergic interneurons (Figures S7D–S7F) and some expressed CALBINDIN (Figure S7G), suggesting a GABAergic phenotype. These observations suggest that reprogramming and survival of iNs following transplantation are affected by both the origin of the reprogrammed cell and TF used.

CerebAstro and CtxAstro iNs Integrate as Olfactory Bulb Interneurons upon Transplantation in the SVZ

Next, we set out to test whether integration of iNs could be facilitated by transplantation into a neurogenic milieu. Toward this aim, we transplanted CerebAstro and CtxAstro in the SVZ of postnatal animals following their nucleofection with either ASCL1 or dsRed. Thirty days after transplantation, we observed a substantial number of GFP$^+$ cells in the rostral migratory stream (RMS) and olfactory bulb (OB) of host animals (Figures 6A–6F). In the control group, virtually all GFP$^+$ cells nucleofected with control plasmid retained astrocytic morphologies in the SVZ, RMS, and OB (Figures S7P–S7Q, n > 300 cells). In contrast, a significant fraction of CtxAstro and CerebAstro nucleofected with ASCL1 adopted morphologies typical of bona fide OB neurons. Notably, iNs adopted typical morphologies of neurons of the granule cell layer (GCL) or periglomerular (PGL) (Figures 6H–6U) and expressed the mature neuronal marker NEUN (Figures 6Q and 6R). However, the ratio of iNs in the GCL and PGL varied depending on the reprogrammed astroglia (Figure 6G). While iNs derived from

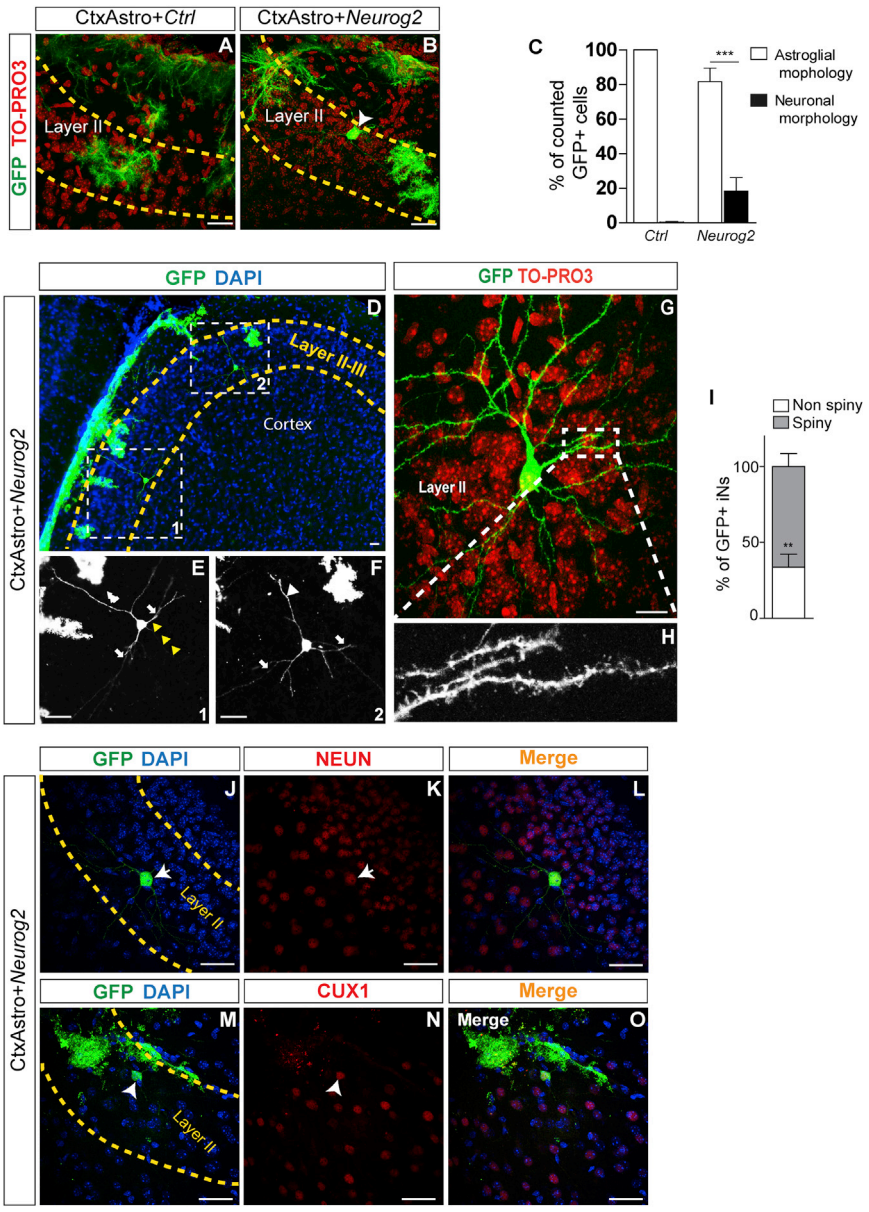

Figure 5. Cortical Astroglia Nucleofected with NEUROG2 Integrate as Pyramidal Cell-like iNs In Vivo

(A and B) Examples of GFP$^+$ CtxAstro 20 days post transplantation (dpt) in the postnatal mouse cerebral cortex. Observe the astrocytic morphology of CtxAstro nucleofected with control plasmid (Ctrl) in the cortical layer II (A), and the presence of GFP$^+$ cells with neuronal morphology in animals transplanted with CtxAstro nucleofected with NEUROG2 (B, arrowhead).

(C) Quantification of cells showing astroglial or neuronal morphology 20 days after transplantation. ***$p < 0.001$.

(D–H) Examples of GFP$^+$ pyramidal-like iNs observed in the cerebral cortex following transplantation of CtxAstro nucleofected with NEUROG2. Note the typical pyramidal cell morphology of iNs in layers II and III of the host cerebral cortex (D, dashed boxes). (E and F) Magnification of dashed boxes shown in (D) revealing the apical dendrite (white arrowheads), basal dendrites (white arrows), and axonal process of iNs (yellow arrowheads). (G) Example of iN in layer II of the cerebral cortex showing spiny dendrites (dashed box magnified in H), suggestive of a glutamatergic identity.

(I) Quantification of spiny and non-spiny iNs in the cerebral cortex of host animals. **$p < 0.01$.

(J–L) GFP$^+$ iN 20 dpt expressing the mature neuronal marker NEUN (J and K, white arrows).

(M–O) GFP$^+$ iN 20 dpt expressing the transcription factor CUX1 (M–N, white arrowheads). Nuclei are stained with either DAPI (blue) or TO-PRO3 (red).

Statistical test in (C) and (I): Student's t test (mean ± SEM). n = 5 animals/condition. WM, white matter. Scale bars, 50 μm. See also Figure S7.

CtxAstro mostly adopted the fate of GCL neurons (types I and III) (CtxAstro$^+$ ASCL1: 68% ± 14%, n = 117 cells; CerebAstro$^+$ ASCL1: 28% ± 10%, n = 87 cells), iNs derived from CerebAstro preferentially integrated as PGL neurons (CerebAstro$^+$ ASCL1: 71% ± 10%; CtxAstro$^+$ ASCL1: 31% ± 14%). We also observed a small number of iNs with granular- and periglomerular-like morphologies after transplantation of CtxAstro nucleofected with NEUROG2 in the SVZ (Figures S7R–S7S). Notably, the expression of calcium binding proteins in OB iNs was different from that observed in vitro (Figure 4). We could not observe PARV$^+$ iNs or CALB$^+$ iNs in the OB after transplantation of both CerebAstro and CtxAstro in the postnatal SVZ (Figures 6S–6U and data not shown).

Finally, we transplanted ASCL1 lineage-reprogrammed CtxAstro in the adult SVZ. We observed that, similar to our experiments in the postnatal brain, GFP cells also migrated throughout the RMS and reached the OB (Figure 7). However, many cells, albeit with neuronal morphology, remained in the RMS (Figures 7C, 7D, and 7H). Among the cells that differentiate within the OB, we observed exclusively iNs in the GCL with morphologies of granular neurons (Figures 7A, 7E, and 7H, 58.9% ± 8%, n = 98 counted cells, n = 2 animals).

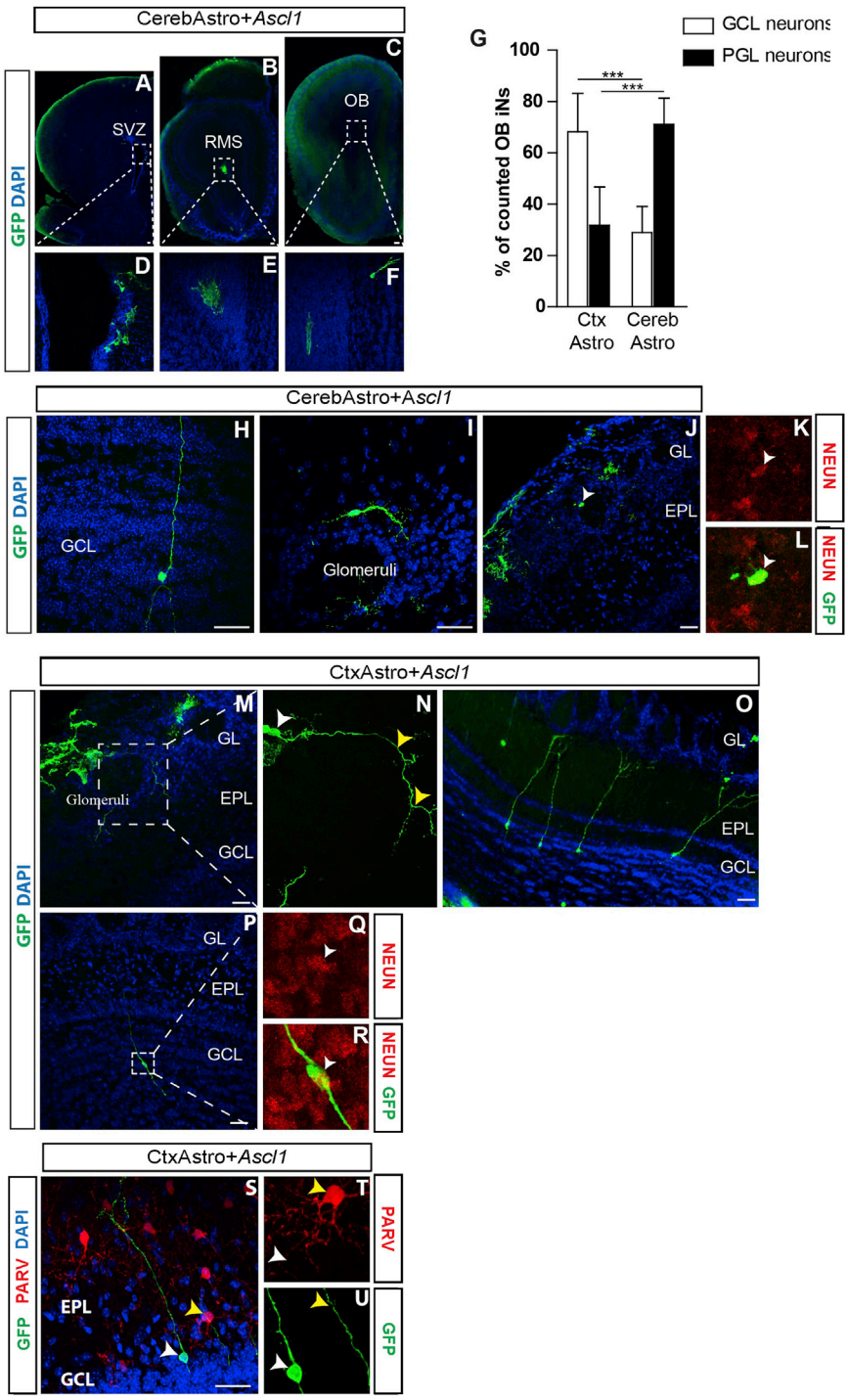

Figure 6. Cerebellar and Cortical Astroglia-Derived iNs Integrate in the Postnatal Olfactory Bulb

(A–F) Coronal sections obtained from a mouse brain 30 dpt of CerebAstro nucleofected with ASCL1. GFP$^+$ cells grafted in the SVZ (A), anterior RMS (B), and OB (C). Dashed boxes in (A) to (C) are magnified in (D) to (F).

(G) Quantification of iNs in the GCL or PGL of the OB following transplantation of CerebAstro or CtxAstro nucleofected with ASCL1 in the SVZ. ***$p < 0.001$.

(H–L) Examples of GFP$^+$ OB iNs derived from CerebAstro nucleofected with ASCL1. Note the typical morphology of granular (H) or periglomerular (I) OB neuron adopted by iNs. Observe also the expression of NEUN (J–L, white arrowhead).

(M–R) Examples of GFP$^+$ iNs in the OB, derived from CtxAstro nucleofected with ASCL1. Observe the typical morphologies of iNs in the PGL (N, white arrowhead points to the cell soma and yellow arrowheads indicate the processes of the same cell) and GCL (O and P). (Q and R) Example of a granular-like iN expressing NEUN (white arrowheads).

(S) Immunohistochemistry for PARV (red) and GFP (green) in the OB of a transplanted animal.

(T and U) Magnification of cells in (S): PARV$^+$ cell (yellow arrowheads), GFP$^+$/PARV$^-$ iNs (white arrowheads).

PARV, PARVALBUMIN; SVZ, subventricular zone; RMS, rostral migratory stream; OB, olfactory bulb; GL, glomerular layer; EPL, external plexiform layer; GCL, granule cell layer. Nuclei are stained with DAPI (blue). Statistical test: two-way ANOVA followed by Bonferroni post hoc test (mean ± SEM). N = 5 animals/condition.

Scale bars, 50 μm. See also Figure S7.

Some of these cells expressed GABA (Figures 7F and 7G). Still different from transplantation in the postnatal SVZ, we did not detect GFP$^+$ cells with astroglial morphology in the OB following transplantation of CtxAstro in the adult SVZ.

Altogether, these data suggest that the neurogenic environment in the SVZ plays an instructive role in the phenotypic specification of iNs. However, the origin of astroglial cells and the TF used for reprogramming interfere with the final fate of iNs.

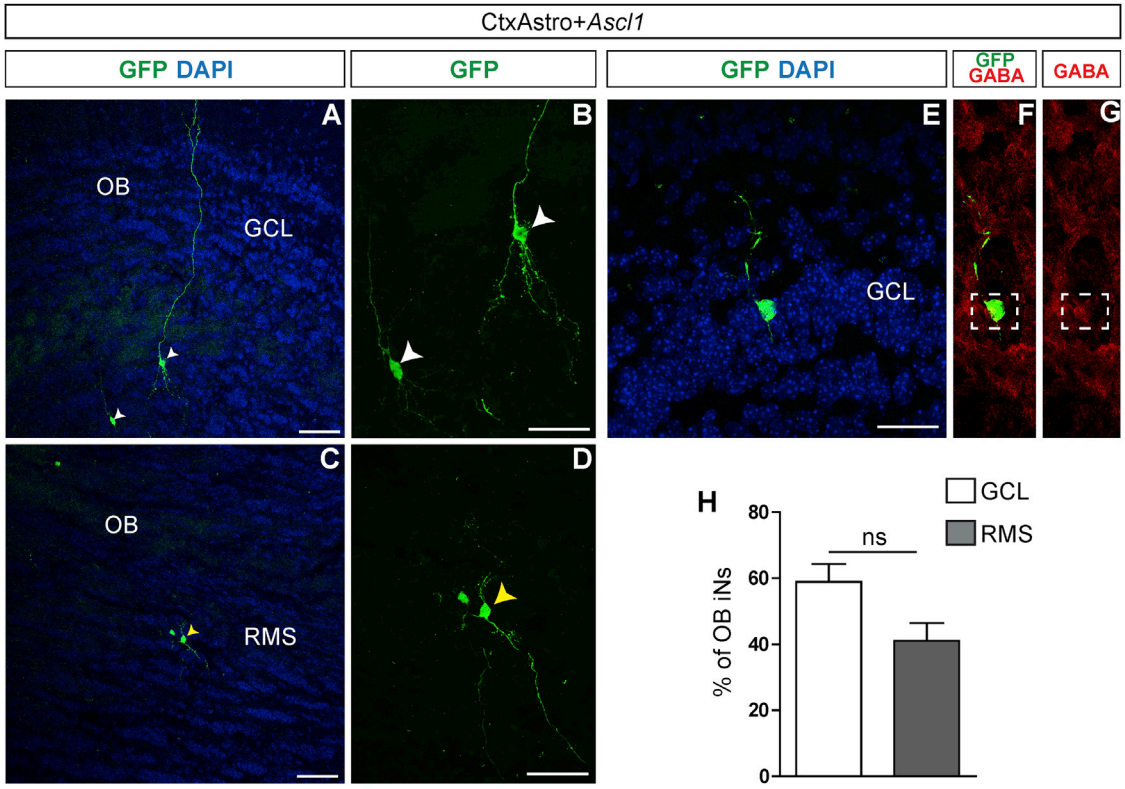

Figure 7. Cortical Astroglia Are Reprogrammed into iNs in the Adult SVZ-RMS-OB

(A–G) Immunostainings showing GFP$^+$ CtxAstro nucleofected with ASCL1 30 dpt in the adult SVZ. Example of granular cell-like iNs observed in the OB (A, white arrowheads; magnified in B). Example of iNs found in the anterior RMS (C, yellow arrowhead; magnified in D). Example of GFP$^+$ granular cell-like iN expressing GABA (E–G).

(H) Quantification of iNs located in the GCL (white bar) or RMS (gray bar) 30 dpt (Student's t test, mean ± SEM).

GCL, granule cell layer; RMS, rostral migratory stream; OB, olfactory bulb; ns, not significant. Nuclei are stained with DAPI (blue). n = 3 animals/condition.

Scale bars, 50 μm.

DISCUSSION

Here we show that, similar to their CtxAstro counterparts, postnatal CerebAstro can be efficiently lineage reprogrammed into functional iNs using a single TF. More importantly, we reveal that astroglial cells isolated from different regions and reprogrammed by overexpression of NEUROG2 or ASCL1 generate iNs with different morphological and neurochemical phenotypes. Finally, we demonstrate that integration of iNs after transplantation depends on several factors such as the origin of astroglia population, the TF used, the region of transplant, and the age of the transplanted animal.

Studies focused on astroglial cells reprogramming into neurons exclusively used CtxAstro as starting cell population (Berninger et al., 2007; Heinrich et al., 2010). However, it remained unclear whether astroglial cells isolated from other regions of the CNS could be reprogrammed into iNs using the same TFs. Here, we show that postnatal cerebellum astroglia can be reprogrammed into neurons following overexpression of NEUROG2 or ASCL1 at rates similar to those observed in postnatal cortical astroglia. This study therefore extended neurogenic potential to cerebellum astroglia, suggesting that neurogenic potential may be a hallmark of every astroglia population of the CNS. We chose to use cerebellum because NEUROG2 and ASCL1 lineages contribute different neuronal phenotypes compared with the cerebral cortex.

In fact, ASCL1 and NEUROG2 are TFs belonging to the basic helix-loop-helix family and expressed in different regions of the developing CNS. In the telencephalon, ASCL1 is mostly expressed by progenitors in the ganglionic eminences and contributes to the generation of cortical GABAergic neurons, whereas NEUROG2 is mostly expressed by dorsal progenitors that generate glutamatergic neurons (Fode et al., 2000; Parras et al., 2002; Schuurmans

and Guillemot, 2002). These developmental roles of TFs have been suggested to explain the phenotype of lineage-reprogrammed CtxAstro iNs (Heinrich et al., 2010). However, the very same TFs are expressed by progenitors contributing inhibitory interneurons and Purkinje cells of the cerebellar cortex (Zordan et al., 2008; Kim et al., 2008).

According to these roles in the developing cerebellum, we show that ASCL1 and NEUROG2 reprogram CerebAstro mostly into GABAergic iNs. Moreover, expression of calcium binding proteins reveals that ASCL1 and NEUROG2 lineage-reprogrammed CerebAstro iNs are distinct: while ASCL1 induces mostly CALBINDIN expression, NEUROG2 induces PARVALBUMIN. These observations are in line with previous suggestions of these TFs instructing distinct neuronal phenotypes in the developing cerebellum (Zordan et al., 2008). Moreover, we observed that most iNs displaying complex morphologies after ASCL1 also expressed CALBINDIN and CTIP2, which are typical hallmarks of Purkinje cells.

Electrophysiological recordings of CerebAstro-derived iNs indicate similarities and possible differences to CtsAstro-derived iNs. In fact, resting membrane potential, action potential amplitudes, and input resistance of CerebAstro-derived iNs are similar to values previously reported to CtxAstro-derived iNs (Berninger et al., 2007). However, ASCL1 expression in CerebAstro induces the generation of 30% regular spiking iNs, whereas no regular spiking iNs could be observed in CtxAstro reprogrammed with ASCL1 and Dlx2 (Heinrich et al., 2010). Future experiments should systematically compare the electrophysiological properties of iNs generated from distinct astroglia, reprogrammed with different TFs.

Considering that ASCL1 and NEUROG2 reprogram CtxAstro into iNs adopting mostly a GABAergic or glutamatergic phenotype, respectively (Heinrich et al., 2010 and our own data), which is reminiscent of the roles of those TFs in the developing telencephalon, a parsimonious explanation for these data is that astroglial cells retain a molecular memory of the region from where they were isolated. In fact, corroborating this idea, many recent data indicate that reprogrammed somatic cells retain residual DNA methylation signatures characteristic of their somatic tissue of origin. These are called "memory" of origin and indeed favor their differentiation toward lineages related to the donor cells (Hu et al., 2010; Kim et al., 2010; Polo et al., 2010; Tian et al., 2011). Astroglial cells from separate regions of the CNS may present different chromatin modifications in genes targeted by neurogenic TFs. These modifications are likely to occur in early progenitor cells, under influence of distinct morphogenetic signals at different domains of the developing CNS (Kiecker and Lumsden, 2005; Lupo et al., 2006), before generation of neurons and glial cells. This patterning contributes to generate neuronal diversity but would also be inherited by astroglial cells within the same lineage (Costa et al., 2009; Gao et al., 2014). Alternatively, astroglial cells obtained from different regions could express different sets of microRNAs or long non-coding RNAs involved in the specification of neuronal fates (Flynn and Chang, 2014; Jönsson et al., 2015). Future experiments should help to elucidate the exact molecular machinery controlling the acquisition of neuronal phenotypes during lineage reprogramming. It will also be interesting to test whether astroglial cell types isolated from other CNS regions, such as the spinal cord and retina, generate iNs phenotypically similar to neurons of these regions.

In accordance with our observations in vitro, iNs derived from NEUROG2 lineage-reprogrammed CtxAstro and transplanted in the postnatal cerebral cortex mostly adopted a phenotype of pyramidal spiny neurons, which are glutamatergic in this region (Shepherd, 2003). Similarly, previous data in the literature have shown that NEUROD1, a downstream target of NEUROG2, converts cerebral cortex reactive astrocytes into $TBR1^+$ iNs in situ (Guo et al., 2014). However, iNs morphologies described here are much more elaborate, showing typical apical and basal dendrites as well as long-distance axonal projections. One possible explanation for this thorough differentiation of iNs could be that NEUROG2 targets genes important for morphological maturation of cortical pyramidal cells that are not regulated by NEUROD1. In fact, it has been shown that phosphorylation of a single tyrosine residue (T241) of NEUROG2 is necessary and sufficient to control radial migration, neuronal polarity and dendritic morphology of pyramidal neurons (Hand et al., 2005). We assume that NEUROG2 phosphorylation happens in grafted iNs within the host-developing cortex and therefore permits the development of a mature pyramidal morphology. In contrast, however, CerebAstro expressing NEUROG2 and transplanted in the postnatal cerebral cortex differentiate into a very small number of iNs with GABAergic interneuron phenotypes. Thus, NEUROG2 expression alone is not sufficient to reprogram all astroglial populations into pyramidal-like iNs in vivo. Finally, we found very few cells with GABAergic interneuron-like morphologies in the cerebral cortex of animals transplanted with cortical or cerebellum or cerebral cortex astroglia nucleofected with ASCL1, further supporting the notion that both the origin of the astroglial cell and the TF used for reprogramming are important in determining the final fate of iNs in vivo.

The environment in the postnatal cerebral cortical may not be permissive for all lineage-reprogrammed astroglial cells to differentiate into iNs. In fact, after transplantation in the neurogenic subventricular zone, we observed that both cerebellar and cortical astroglia nucleofected with ASCL1 could migrate throughout the RMS and differentiate in the OB as GCL- and PGL-like interneurons. This suggests that the milieu in the postnatal SVZ is not only more permissive to lineage-reprogrammed astroglia iNs, but also plays instructive roles in

the phenotype of the iNs. Interestingly, however, despite this instructive role of environment, ASCL1 lineage-reprogrammed cortical and cerebellar astroglia iNs generated GCL- and PGL-like interneurons at different ratios, suggesting that the origin of the astroglial cell still play some role in fate determination. A few iNs were also detected in the OB after transplantation of cortical astroglia nucleofected with NEUROG2. One possible explanation for this difference could be the distinct roles played by ASCL1 and NEUROG2 in the postnatal SVZ. While the former is required for generation of most OB interneurons, especially granule cells (Parras et al., 2004), NEUROG2 contributes to the generation of a very small proportion of juxtaglomerular neurons (Winpenny et al., 2011).

Of note, we observed GFP$^+$ cells with astrocytic morphologies in the RMS and OB of all animals transplanted with both cortical and cerebellar astroglia at postnatal stages, regardless of the plasmid used for transfection (*control-*, *Neurog2-*, or *Ascl1-DsRed*). Most of these cells did not express dsRed (non-transfected cell) and some did (transfected but not reprogrammed). This observation suggests that transplanted astrocytic cells can also respond to migration cues in the SVZ-RMS-OB system and integrate in the OB. Accordingly it has been recently shown that astrocytes are constantly added to the OB after generation in the SVZ (Sohn et al., 2015).

Finally, we also observed that integration in the adult brain is more limited than in the postnatal brain. In fact, we could not observe integration of iNs after transplantation in the adult cerebral cortex (data not shown). In the adult OB we could detect some iNs following transplantation of cortical astroglia transfected with ASCL1. Interestingly, an important fraction of iNs in the adult OB seems to have a problem in reaching the GCL.

Altogether, our results indicate that lineage reprogramming of astroglial cells into neurons by neurogenic TFs is more complex than previously thought. In fact, they show that a same TF can induce the generation of glutamatergic or GABAergic iNs, which would have a completely different role in a neuronal circuitry. Moreover, they demonstrate that both the origin and the region of integration play an important role in the phenotypic specification of iNs. These results have critical relevance for future cell-based therapies, using either transplantation of exogenous lineage-reprogrammed astroglial cells or direct in situ lineage reprogramming of resident astroglia.

EXPERIMENTAL PROCEDURES

Astroglia Culture and Nucleofection

Postnatal CerebAstro and CtxAstro were isolated from mice on P5–P7. Cerebral cortex gray matter and entire cerebellum were removed and mechanically dissociated. Tissues from both regions were plated separately in culture flasks containing Astromedium (see Supplemental Experimental Procedures). After 3–4 days, medium was replaced with fresh Astromedium. After confluence, astroglial cells were nucleofected with pCAG-*Neurog2*-IRES-*DsRed*, pCAG-*Ascl1*-IRES-*DsRed*, or the control plasmid pCAG-IRES-*DsRed* using 4D nucleofector (LONZA) (see Supplemental Experimental Procedures). Next, cells were plated at densities from 7×10^4 to 1×10^5 cells/well on poly-D-lysine-coated 24-well tissue plates containing serum-free differentiation medium. For some experiments, primary cells isolated from the neonatal brain were co-cultured at 5 days post nucleofection (see Supplemental Experimental Procedures).

Cell Transplantation

CerebAstro and CtxAstro were isolated from postnatal GFP animals and cultured as described above. After nucleofection, cells were counted, suspended in serum-free DMEM-F12 (Gibco) at 3–5 $\times$ 10^5 cells/μL, and maintained on ice until transplantation procedure. One microliter of cell suspension was gently injected using a pulled glass capillary coupled to a manual injector in the cerebral cortex or SVZ of P0–P2 C57BL/6 mice anesthetized by hypothermia. Transplantation in young adults (P30–P60) C57BL/6 mice were performed under isoflurane anesthesia. Cells were injected using a nanoinjector (Nanoliter 2010, WPI) coupled to a glass capillary using the following stereotactic coordinates (in mm): SVZ (anteroposterior [AP], 0.6; mediolateral [MV], 1.2; dorsoventral [DV], 1.8) and cortex (AP, 1.58; ML, 3.44; DV, 1.40).

Quantifications and Statistical Analysis

Quantification of neuronal reprogramming and iNs phenotype in vitro was performed in at least three independent batches of cell culture. For the transplantation studies in the postnatal brain, we analyzed three to five animals for each condition (type of astroglial cell, TF used, and region of grafting). Total number of cells analyzed is described throughout the text (see also Supplemental Experimental Procedures). Statistical tests were performed using GraphPad Prism version 5.00 for Windows (www.graphpad.com). Confidence interval is 95%. Statistical significance is indicated in the figures as follows: *$p < 0.05$; **$p < 0.01$; ***$p < 0.001$.

SUPPLEMENTAL INFORMATION

Supplemental Information includes Supplemental Experimental Procedures, seven figures, one table, and four movies and can be found with this article online at http://dx.doi.org/10.1016/j.stemcr.2017.05.009.

AUTHOR CONTRIBUTIONS

M.C. and M.R.C. designed the work, collected and analyzed data, and wrote the article. A.R.M.F. and D.M.S.M. performed video-microscopy time-lapse and fate-mapping experiments. M.M.H. and R.N.L. performed electrophysiological recordings. T.S. provided the software for acquisition and analysis of time-lapse video microscopy experiments. All authors read and approved the final version of the article.

ACKNOWLEDGMENTS

This work was supported by CNPq (MRC 473254/2013-1 and 466959/2014-1) and CAPES fellowships to M.C. and D.M. We thank Dr. Benedikt Berninger for providing the plasmids encoding for proneural factors and for helpful discussion of the manuscript. We also thank Dr. Cecilia Hedin Pereira, Dr. Cláudio Queiroz, Dra. Katarina Leão, and Dr. Ricardo Reis for valuable discussion of the work, and Rebecca Diniz, Ana Cristina, and Giovanna Andrade for technical assistance.

Received: April 19, 2016
Revised: May 8, 2017
Accepted: May 9, 2017
Published: June 8, 2017

REFERENCES

Arlotta, P., and Berninger, B. (2014). Brains in metamorphosis: reprogramming cell identity within the central nervous system. Curr. Opin. Neurobiol. *27*, 208–214.

Barnes, A.P., and Polleux, F. (2009). Establishment of axon-dendrite polarity in developing neurons. Annu. Rev. Neurosci. *32*, 347–381.

Berninger, B., Costa, M.R., Koch, U., Schroeder, T., Sutor, B., Grothe, B., et al. (2007). Functional properties of neurons derived from in vitro reprogrammed postnatal astroglia. J. Neurosci. *27*, 8654–8664.

Costa, M.R., Bucholz, O., Schroeder, T., and Götz, M. (2009). Late origin of glia-restricted progenitors in the developing mouse cerebral cortex. Cereb. Cortex *19*, i135–i143.

Emsley, J.G., and Macklis, J.D. (2006). Astroglial heterogeneity closely reflects the neuronal-defined anatomy of the adult murine CNS. Neuron Glia Biol. *2*, 175–186.

Flynn, R.A., and Chang, H.Y. (2014). Long noncoding RNAs in cell-fate programming and reprogramming. Cell Stem Cell *14*, 752–761.

Fode, C., Ma, Q., Casarosa, S., Ang, S.-L., Anderson, D.J., and Guillemot, F. (2000). A role for neural determination genes in specifying the dorsoventral identity of telencephalic neurons. Genes Dev. *14*, 67–80.

Gao, P., Postiglione, M.P., Krieger, T.G., Hernandez, L., Wang, C., Han, Z., et al. (2014). Deterministic progenitor behavior and unitary production of neurons in the neocortex. Cell *159*, 775–788.

Gascón, S., Murenu, E., Masserdotti, G., Ortega, F., Russo, G.L., Petrik, D., et al. (2015). Identification and successful negotiation of a metabolic checkpoint in direct neuronal reprogramming. Cell Stem Cell *18*, 396–409.

Guo, Z., Zhang, L., Wu, Z., Chen, Y., Wang, F., and Chen, G. (2014). In vivo direct reprogramming of reactive glial cells into functional neurons after brain injury and in an Alzheimer's Disease model. Cell Stem Cell *14*, 188–202.

Hand, R., Bortone, D., Mattar, P., Nguyen, L., Heng, J.I.T., Guerrier, S., et al. (2005). Phosphorylation of neurogenin2 specifies the migration properties and the dendritic morphology of pyramidal neurons in the neocortex. Neuron *48*, 45–62.

Heinrich, C., Blum, R., Gascón, S., Masserdotti, G., Tripathi, P., Sánchez, R., et al. (2010). Directing astroglia from the cerebral cortex into subtype specific functional neurons. PLoS Biol. *8*, e1000373.

Heinrich, C., Spagnoli, F.M., and Berninger, B. (2015). In vivo reprogramming for tissue repair. Nat. Cell Biol. *17*, 204–211.

Hevner, R.F., Hodge, R.D., Daza, R.A.M., and Englund, C. (2006). Transcription factors in glutamatergic neurogenesis: conserved programs in neocortex, cerebellum, and adult hippocampus. Neurosci. Res. *55*, 223–233.

Hu, Q., Friedrich, A.M., Johnson, L.V., and Clegg, D.O. (2010). Memory in induced pluripotent stem cells: reprogrammed human retinal-pigmented epithelial cells show tendency for spontaneous redifferentiation. Stem Cells *28*, 1981–1991.

Hu, W., Qiu, B., Guan, W., Wang, Q., Wang, M., Li, W., et al. (2015). Direct conversion of normal and Alzheimer's disease human fibroblasts into neuronal cells by small molecules. Cell Stem Cell *17*, 204–212.

Hvalby, Ø., Jensen, V., Kao, H.T., and Walaas, S.I. (2006). SYNAPSIN-regulated synaptic transmission from readily releasable synaptic vesicles in excitatory hippocampal synapses in mice. J. Physiol. *571*, 75–82.

Jönsson, M.E., Wahlestedt, J.N., Åkerblom, M., Kirkeby, A., Malmevik, J., Brattaas, P.L., et al. (2015). Comprehensive analysis of microRNA expression in regionalized human neural progenitor cells reveals microRNA-10 as a caudalizing factor. Development *142*, 3166–3177.

Kiecker, C., and Lumsden, A. (2005). Compartments and their boundaries in vertebrate brain development. Nat. Rev. Neurosci. *6*, 553–564.

Kim, E.J., Battiste, J., Nakagawa, Y., and Johnson, J.E. (2008). ASCL1 (Mash1) lineage cells contribute to discrete cell populations in CNS architecture. Mol. Cell. Neurosci. *38*, 595–606.

Kim, K., Doi, A., Wen, B., Ng, K., Zhao, R., Cahan, P., et al. (2010). Epigenetic memory in induced pluripotent stem cells. Nature *467*, 285–290.

Laywell, E.D., Rakic, P., Kukekov, V.G., Holland, E.C., and Steindler, D.A. (2000). Identification of a multipotent astrocytic stem cell in the immature and adult mouse brain. Proc. Natl. Acad. Sci. USA *97*, 13883–13888.

Leid, M., Ishmael, J.E., Avram, D., Shepherd, D., Fraulob, V., and Dollé, P. (2004). CTIP1 and CTIP2 are differentially expressed during mouse embryogenesis. Gene Expr. Patterns *4*, 733.

Lupo, G., Harris, W.A., and Lewis, K.E. (2006). Mechanisms of ventral patterning in the vertebrate nervous system. Nat. Rev. Neurosci. *7*, 103–114.

Masserdotti, G., Gillotin, S., Sutor, B., Drechsel, D., Irmler, M., Jørgensen, H.F., et al. (2015). Transcriptional mechanisms of proneural factors and rest in regulating neuronal reprogramming of astrocytes. Cell Stem Cell *17*, 74–88.

Niu, W., Zang, T., Zou, Y., Fang, S., Smith, D.K., Bachoo, R., et al. (2013). In vivo reprogramming of astrocytes to neuroblasts in the adult brain. Nat. Cell Biol. *15*, 1164–1175.

Niu, W., Zang, T., Smith, D.K., Vue, T.Y., Zou, Y., Bachoo, R., et al. (2015). SOX2 reprograms resident astrocytes into neural progenitors in the adult brain. Stem Cell Reports *4*, 780–794.

Okabe, M., Ikawa, M., Kominami, K., Nakanishi, T., and Nishimune, Y. (1997). 'Green mice' as a source of ubiquitous green cells. FEBS Lett. *407*, 313–319.

Pang, Z.P., Yang, N., Vierbuchen, T., Ostermeier, A., Fuentes, D.R., Yang, T.Q., et al. (2011). Induction of human neuronal cells by defined transcription factors. Nature *476*, 220–223.

Parras, C.M., Schuurmans, C., Scardigli, R., Kim, J., Anderson, D.J., and Guillemot, F. (2002). Divergent functions of the proneural genes Mash1 and Ngn2 in the specification of neuronal subtype identity. Genes Dev. *16*, 324–338.

Parras, C.M., Galli, R., Britz, O., Soares, S., Galichet, C., Battiste, J., et al. (2004). Mash1 specifies neurons and oligodendrocytes in the postnatal brain. EMBO J. *23*, 4495–4505.

Polo, J.M., Liu, S., Figueroa, M.E., Kulalert, W., Eminli, S., Tan, K.Y., et al. (2010). Cell type of origin influences the molecular and functional properties of mouse induced pluripotent stem cells. Nat. Biotechnol. *28*, 848–855.

Schuurmans, C., and Guillemot, F. (2002). Molecular mechanisms underlying cell fate specification in the developing telencephalon. Curr. Opin. Neurobiol. *12*, 26–34.

Shepherd, G.M. (2003). The Synaptic Organization of the Brain (Oxford University Press).

Sohn, J., Orosco, L., Guo, F., Chung, S.-H., Bannerman, P., Ko, E.M., et al. (2015). The subventricular zone continues to generate corpus callosum and rostral migratory stream astroglia in normal adult mice. J. Neurosci. *35*, 3756–3763.

Takano, T., Xu, C., Funahashi, Y., Namba, T., and Kaibuchi, K. (2015). Neuronal polarization. Development *142*, 2088–2093.

Tian, C., Wang, Y., Sun, L., Ma, K., and Zheng, J.C. (2011). Reprogrammed mouse astrocytes retain a "memory" of tissue origin and possess more tendencies for neuronal differentiation than reprogrammed mouse embryonic fibroblasts. Protein Cell *2*, 128–140.

Victor, M.B., Richner, M., Hermanstyne, T.O., Ransdell, J.L., Sobieski, C., Deng, P.Y., et al. (2014). Generation of human striatal neurons by microRNA-dependent direct conversion of fibroblasts. Neuron *84*, 311–323.

Vierbuchen, T., Ostermeier, A., Pang, Z.P., Kokubu, Y., Südhof, T.C., and Wernig, M. (2010). Direct conversion of fibroblasts to functional neurons by defined factors. Nature *463*, 1035–1041.

Whitford, K.L., Dijkhuizen, P., Polleux, F., and Ghosh, A. (2002). Molecular control of cortical dendrite development. Annu. Rev. Neurosci. *25*, 127–149.

Winpenny, E., Lebel-Potter, M., Fernandez, M.E., Brill, M.S., Götz, M., Guillemot, F., and Raineteau, O. (2011). Sequential generation of olfactory bulb glutamatergic neurons by NEUROG2-expressing precursor cells. Neural Dev. *6*, 2.

Zordan, P., Croci, L., Hawkes, R., and Consalez, G.G. (2008). Comparative analysis of proneural gene expression in the embryonic cerebellum. Dev. Dyn. *237*, 1726–1735.

Stem Cell Reports, Volume *9*

Supplemental Information

Lineage Reprogramming of Astroglial Cells from Different Origins into Distinct Neuronal Subtypes

Malek Chouchane, Ana Raquel Melo de Farias, Daniela Maria de Sousa Moura, Markus Michael Hilscher, Timm Schroeder, Richardson Naves Leão, and Marcos Romualdo Costa

Supplemental information to the manuscript *"Lineage reprogramming of astroglial cells from different origins into distinct neuronal subtypes"* by Chouchane et al.

Supplemental Experimental Procedures

Animals

We used C57BL/6, actin-GFP (Okabe et al., 1997), GAD67-GFP (Tamamaki et al., 2003), PV-Cre (Tanahira et al., 2009), GLAST-CreERT2 (Mori et al., 2006) and CAG-CAT-GFP mice (Nakamura et al., 2006). All procedures were done in accordance with national and international laws and were approved by the local ethical committee (CEUA/UFRN, license # 008/2014).

Isolation and expansion of astroglial cells

Cerebellum and cerebral cortex tissues were mechanically triturated and plated in T75 culture flasks containing Astromedium, composed of DMEM/F12 (Gibco), 3.5 mM glucose (Sigma), 10% fetal bovine serum (Gibco), 5% horse serum (Gibco), 100U/ml penicillin/streptomycin (Gibco), 2 % B27 (Gibco), 10 ng/mL epidermal growth factor (EGF, Gibco) and 10ng/mL fibroblast growth factor 2 (FGF2, Gibco). Cultures were incubated at 5% CO_2 and 37°C without moving. After 3-4 days, cultures were washed vigorously with PBS in order to remove unattached and weakly attached cells and medium was replaced with fresh Astromedium. After 7-10 days, astroglial cells reached up to 90% of confluence and were used for transfection.

Astroglial cell passage and transfection

Astroglial cells were chemically detached from T75 culture flasks using trypsin/EDTA (Gibco) 0,5% for 10 minutes at 37^{o}C. In order to stop trypsin action, an equal amount of medium with

10% FBS was added to the detaching cells. Cells were then centrifuged at 1500rpm, 4ºC for 5 min. To generate subsequent passages, 10^6 cells were plated in T75 culture flasks containing Astromedium. Between each passage, the total number of cells was counted, allowing the calculation of the growth rate. For the neurosphere assay, $5x10^5$ were plated in T25 culture flasks containing 5 ml neurosphere medium, composed of DMEM/F12 (Gibco), 3.5 mM glucose (Sigma), 100U/ml penicillin/streptomycin (Gibco), 2% B27 (Gibco), 10 ng/mL epidermal growth factor (EGF, Gibco) and 10ng/mL fibroblast growth factor 2 (FGF2, Gibco). After 7 days, neurospheres were dissociated using trypsin/EDTA (Gibco) 0,5% for 10 minutes at 37^{o}C. Dissociated cells were then plated onto PDL-coated glass coverslips in neurosphere medium without growth factors. For nucleofection, cells were resuspended at 5 x 10^4 cells/µl in the P3 solution (Lonza) containing 1-2 µg of plasmid DNA. Cell/DNA suspension was dropped in the nucleofection well to receive an electrical shock with the program EM110 for mammalian glial cells (Lonza). Astroglial cells were nucleofected with either *pCAG-Neurog2-IRES-DsRed*, *pCAG-Ascl1-IRES-DsRed* or the control plasmid *pCAG-IRES-DsRed*. Next, cells were plated at a density of 70.000 to 100.000 cells/well in poly-D-lysine coated 24-well tissue plates containing Astromedium. 24 hours after nucleofection, medium was replaced with differentiation medium composed of DMEM/F12, 3.5 mM glucose, penicillin/streptomycin and 2% B27. Brain-derived neurotrophic factor (BDNF, Sigma) was added at 20ng/mL every fifth day during the differentiation process.

Co-culture of lineage-reprogrammed astroglial cells with hippocampal neurons

Due to the decreasing survival rate of iNs starting from 20 days post transfection, for analyses performed after this period we co-cultured transfected cells 5 days after nucleofection with hippocampal neurons isolated from P0 pups. Briefly, hippocampal tissues were dissected and

dissociated in trypsin/ EDTA for 15 min. Cells were then centrifuged (1000 rpm, 4ºC) and suspended in a serum-containing medium to stop trypsin activity. Next, cells were centrifuged again, suspended in serum-free medium and added at a density of 50.000 to 70.000 cells/well.

Time-Lapse video microscopy

Time-lapse video microscopy of astroglia cell cultures was performed with a Cell Observer Microscope (Zeiss) at constant conditions of 37°C and 5% CO_2. Phase contrast images were acquired every 10 minutes and fluorescence images every 3h up to 5 days using a 10x phase contrast objective (Zeiss). Acquisition and analysis were preformed using TAT and TTT software, respectively (Hilsenbeck et al., 2016).

Electrophysiology

Cell cultures with induced neurons were transferred to a recording chamber mounted on the stage of a microscope (Zeiss Examiner.A1), equipped with a water immersion x40 objective (Nikon, NA 1.0) and perfused at room temperature, oxygenated with external solution (1 – 1.25 ml/min). Data were acquired using a patch-clamp amplifier Axopatch 200B (Molecular Devices, USA) in current clamp mode, a 16-bit data acquisition card (National Instruments), and WinWCP software implemented by Dr. John Dempster (University of Strathclyde, UK). Patch-pipettes of borosilicate glass capillaries (GC150F-10 Harvard Apparatus) were pulled on a vertical puller (Narishige, Japan) with resistances around 7 MΩ. Pipettes were filled with internal solution (~290 Osm) containing (in mM) 130 K+-gluconate, 7 NaCl , 0.1EGTA, 0.3MgCl2, 0.8 CaCl2, 2 Mg-ATP, 0.5 NaGTP, 10 HEPES, and 2 EGTA (pH 7.2 adjusted with KOH 1M). The external solution (~300 Osm) contained (in mM) 120 NaCl, 3 KCl, 1.2 MgCl2, 2.5 CaCl2, 23 NaHCO3, 5 HEPES, and 11 Glucose (pH 7.4 adjusted with NaOH 1M).

Tissue preparation and histology

Cell cultures were fixed with 4% PFA for 10 minutes at room temperature and stored in PBS. For anti-glutamate staining, we also added 0.3% glutaraldehyde to the fixative solution. Primary antibodies were prepared in a solution of 0.5% Triton X-100, 10% normal goat serum (NGS) and 2% bovine serum albumin (BSA). Samples were incubated with primary antibody solution at 4ºC overnight. The following primary antibodies were used: polyclonal anti-green fluorescent protein (GFP, chicken, 1:500, Aves Labs, GFP-1020), polyclonal anti-Glial Fibrillary Acidic Protein (GFAP, rabbit, 1:4000, DakoCytomation, Z0334), polyclonal anti-Red Fluorescent Protein (RFP, rabbit, Rockland, 1:1000, 600-401-379), monoclonal anti-Microtubule Associated Protein 2 (MAP2, mouse IgG1, 1:200, Sigma-Aldrich, M4403), monoclonal anti-NEUN (mouse, 1:500, Millipore, MAB377), monoclonal anti-SYNAPSIN 1 (mouse IgG2, 1:2000, Synaptic Systems, 106001), polyclonal anti-TBR1 (rabbit, 1:500, Abcam, ab51502), monoclonal anti-BIII TUBULIN (mouse IgG2b, 1:500, Sigma, T5076), monoclonal anti-CALBINDIN 28K (mouse IgG1, 1:2000, Swant), monoclonal anti-PARVALBUMIN (mouse IgG1, 1:2000, Sigma, p3088), monoclonal anti-CUX1 (mouse IgG1, 1:500, ABCAM). For some nuclear staining, TO-PRO-3 (1:2000, Invitrogen) was incubated together with secondary antibody solution. After washing with PBS cells were incubated with appropriate species secondary AlexaFluor (Invitrogen) antibodies for 2 hours at room temperature. After 3 washes in PBS, cell nuclei were stained with DAPI and coverslips were mounted on glass slides with an anti-fading mounting medium (Aqua Poly/Mount).

Tissue fixation was performed 20 to 30 days post transplantation. For that, animals were deeply anesthetized with THIOPENTAX (Cristalia) and transcardially perfused using a ventricular catheter with 0.9% saline solution for 15 min and 4% phosphate-buffered saline-buffered

paraformaldehyde (PFA) for another 15 min. Brains were removed and kept in phosphate-buffered saline (PBS) overnight. The next day, brains were kept in 30% sucrose solution for cryoprotection before freezing procedure. Brains were cut in slices going from 40 to 50µm of thickness using a cryostat (Leica). Subsequently, slices were mounted on gelatin-coated slides and stored at -20ºC until immunohistochemistry (see previous paragraph).

Quantifications

For cerebellar astroglia cell culture characterization we counted 2254 cells for GFAP and BIII-TUBULIN immunoreactivity through 3 independent experiments. A similar number of cells were also checked for Sox2 and O4 immunoreactivity. For the in vitro study, cells were quantified for colocalization of DSRED and BIII-TUBULIN immunoreactivity at 7 days post nucleofection (dpn) (CerebAstro-ASCL1: 1320 cells; CerebAstro-NEUROG2: 1234 cells; CerebAstro-DSRED: 1000 cells). A similar number of cells were quantified for CtxAstro condition. Colocalization of DSRED, MAP2 and NEUN was performed 15 dpn (CerebAstro-ASCL1: 686 cells; CerebAstro-NEUROG2: 446 cells). CALBINDIN (CerebAstro-ASCL1: 170 cells; CerebAstro-NEUROG2: 118 cells) and PARVALBUMIN (CerebAstro-ASCL1: 120 cells; cerebAstro-NEUROG2: 143 cells) expression were analyzed at 20 dpn whereas expression of GABA (CerebAstro-ASCL1: 68 cells; CerebAstro-NEUROG2: 58 cells), GLUTAMATE (CerebAstro-ASCL1: 52 cells; Cereb-NEUROG2: 53 cells) and SYNAPSIN (>40 cells for each condition) was analyzed later, at 30 dpn. Induced neurons (iNs) or RFP+ neurons terms refer to DSRED+ cells that have a clear neuronal morphology. Neuronal morphology was quantitatively analyzed using the plugin "Sholl Analysis" (version 3.4.5 June 2015) in ImageJ version 1.49 (NIH). Concentric circles were centered at the centroid of the cell body with starting radius of 40 µm and increments of 40 µm. 15 to 20 neurons were randomly sorted and analyzed in each

group. Neuronal polarity was quantified by counting the number of cell processes within 4 quadrants centered at the soma. In order to compare with CtxAstro, a similar number of cells were counted in each experiment and all results were obtained through at least 3 independent experiments.

For the in vivo experiments, we studied GFP+ cells for their morphology, hodology and neurochemical markers such as NEUN and CUX1. For each transplant, cells were quantified through the entire brain 20 or 30 days post transplantation (see Table S1 for details).

References

Mori, T., Tanaka, K., Buffo, A., Wurst, W., Kuhn, R., and Gotz, M. (2006). Inducible gene deletion in astroglia and radial glia--a valuable tool for functional and lineage analysis. Glia 54, 21-34.

Nakamura, T., Colbert, M.C., and Robbins, J. (2006). Neural crest cells retain multipotential characteristics in the developing valves and label the cardiac conduction system. Circ Res 98, 1547-1554.

Okabe, M., Ikawa, M., Kominami, K., Nakanishi, T., and Nishimune, Y. (1997). 'Green mice' as a source of ubiquitous green cells. FEBS Lett 407, 313-319.

Tamamaki, N., Yanagawa, Y., Tomioka, R., Miyazaki, J., Obata, K., and Kaneko, T. (2003). Green fluorescent protein expression and colocalization with calretinin, parvalbumin, and somatostatin in the GAD67-GFP knock-in mouse. J Comp Neurol 467, 60-79.

Tanahira, C., Higo, S., Watanabe, K., Tomioka, R., Ebihara, S., Kaneko, T., and Tamamaki, N. (2009). Parvalbumin neurons in the forebrain as revealed by PARVALBUMIN-Cre transgenic mice. Neurosci Res 63, 213-223.

Supplemental Table 1

Transplanted cells	Host animals (n)	Age	Injection site	Total of counted cells	Dispersion of cells (µm)	Presence of induced neurons
CtxAstro+DSRED	4	Postnatal	Cortex	1145	400	no
CtxAstro+NEUROG2	5	Postnatal	Cortex	2338	300	yes
CtxAstro+ASCL1	4	Postnatal	Cortex	643	250	few
CerebAstro+DSRED	3	Postnatal	Cortex	500	230	no
CerebAstro+NEUROG2	3	Postnatal	Cortex	756	210	few
CerebAstro+ASCL1	4	Postnatal	Cortex	1020	200	few
CtxAstro+DSRED	3	Postnatal	SVZ	> 100*	3000	no
CtxAstro+NEUROG2	3	Postnatal	SVZ	104*	2610	yes
CtxAstro+ASCL1	4	Postnatal	SVZ	117*	3036	yes
CerebAstro+DSRED	4	Postnatal	SVZ	106*	nd	no
CerebAstro+ASCL1	4	Postnatal	SVZ	87*	3162	yes
CtxAstro+ASCL1	2	Adult	SVZ	98*	3600	yes
CtxAstro+DSRED	2	Adult	SVZ	103*	nd	no

* Only cells in the olfactory bulb.

tx: transplanted, CtxAstro: Cortical astrocytes, CerebAstro: Cerebellar astrocytes.

Supplemental figures legends

Figure S1. ***Related to Figure1*****. Characterization of cerebral cortex and cerebellum astroglial cells cultures and neuronal reprogramming of CtxAstro.** (A-D) Images showing CerebAstro and CtxAstro cell cultures 2h after passage and immunostained for GFAP (A and C, red) and BIII-TUB (B and D, green). Quantification of GFAP+ and BIII-TUB+ cells in both CerebAstro and CtxAstro cultures (E). (F-G) Example of CerebAstro culture 7dpn with DSRED. Note that after 7dpn nucleofected cells fail to express BIII-TUB (G). (H-J) Example of CerebAstro culture 24h after nucleofection with ASCL1. Note that all RFP+ nucleofected cells (I) are GFAP+ (H and J, green). (K-P) CtxAstro cultures 7dpn with DSRED (K-L), ASCL1 (M-N) or NEUROG2 (O-P) and immunostained for BIII-TUB (L, N and P, green). Note RFP+/BIII-TUB+ cells only in cultures nucleofected with ASCL1 (N) or NEUROG2 (P). (Q) Quantification of RFP+/BIII-TUBULIN+ cells amongst all RFP+ cells in CtxAstro 7 dpn with ASCL1 (black bar), NEUROG2 (grey bar) or DSRED (white bar). (R) Scheme explaining experimental procedure for generation of passages 1-4 astrocytes, neurosphere assay and direct lineage reprogramming. (S) Image of cells differentiated from passage 3 (P3) CerebAstro neurospheres. Note that the majority of the cells are GFAP+ (green) and only a very low number of neurons are BIII-TUB+ (red, white arrowhead). (T) Example showing RFP+/BIII-TUB+ ASCL1-iNs derived from passage 4 CerebAstro culture. (U) Table summarizing the results obtained at different passages of CerebAstro and CtxAstro for neurosphere formation, proliferative capacity (measured as mean population doubling time) and reprogramming efficiency. TUB: TUBULIN, N.F: not found, ns: not significant, dpn: days post nucleofection. (Student t-test in Q, Mean±SEM). Nuclei are stained with DAPI (blue). Scale bars: 25µm. 3 independent experiments/condition.

Figure S2. *Related to Figure1*. Time lapse video microscopy shows that postmitotic cerebellum astroglial cells are converted into iNs. (A-J) Fluorescence images of nucleofected cells (arrows) taken from the time lapse series after nucleofection with either *Ascl1-DsRed* (A-D) or *Neurog2-DsRed* (G-J). Same fields can be observed in Supplementary Movies 2 and 3, respectively. (E-L) Post imaging immunohistochemistry showing that nucleofected cells (RFP+) are BIII-TUB+ (E, K). Graph showing the percentage of cell death among nucleofected cells undergoing neuronal conversion (black bar) or remaining in astroglial lineage (white bar). (M) Graph showing the percentage of transfected cells undergoing cell division (N) Time in (A-L) represents days-hours:minutes:seconds. TUB: TUBULIN.

Figure S3. *Related to Figure1*. iNs are directed from cells with astroglial origin. (A) Scheme illustrating experimental design of tamoxifen administration in double-transgenic GLAST-CreERT/CAG-CAT-GFP mice. (B-E) Example of GLAST-GFP astroglial cells culture 15dpn with DSRED. Maximal projection of Z-stacks are shown in B. Single Z-stack of dashed box in B is magnified in C-E. Note that nucleofected cell is GFP+ (C), RFP+ (D) and MAP2- (E). (F-M) Example of fluorescence pictures illustrating GLAST-GFP cells 15 dpn with Ascl1-DsRed (F-I) or Neurog2-DsRed (J-M). Maximal projection of Z-stacks are shown in F and J. Single Z-stacks of dashed boxes in F and J are magnified in G-I and K-M, respectively. Note that cells are GFP+ (G, K), RFP+ (H, L) and MAP2+ (I, M).

Figure S4. Morphological properties of iNs depend on astroglia origin and TF used. (A-D) Fluorescence images illustrating different morphologies of RFP+ (white) iNs derived from CerebAstro (A-B) and CtxAstro (C-D) following nucleofection with ASCL1 (A,C) and NEUROG2 (B, D). Example Of iN (white) plotted on concentric circles (red) for Sholl analysis

(D). Graphs of sholl analysis comparing iNs derived from CerebAstro nucleofected with ASCL1 and NEUROG2 (F), from CerebAstro and CtxAstro nucleofected with ASCL1 (H), from CerebAstro and Ctx Astro nucleofected with NEUROG2 (I) and from CtxAstro nucleofected with ASCL1 or NEUROG2 (J). Cartesian plot representing the polarity of iNs derived from CerebAstro (G) and CtxAstro (K) nucleofected with ASCL1 or NEUROG2. (Two-way ANOVA followed by Bonferroni post test, n>15 iNs/condition, Mean±SEM). Nuclei are stained with DAPI (blue). Scale bars: 100µm (A-D). 3 independent experiments/condition.

Figure S5. ***Related to Figure3*****. Expression of glutamatergic and GABAergic markers in iNs derived from lineage-converted astroglia.** (A-L) Images of CtxAstro and CerebAstro cultures 7 dpn with NEUROG2 (A-I) or ASCL1 (J-L). (A-C) Example of an iN derived from CtxAstro nucleofected with NEUROG2 co-staining for RFP (red) and BIII-TUB (green) and TBR1 (white, arrowhead). (D-F) Example of an iN derived from CerebAstro nucleofected with NEUROG2 co-staining for RFP (red) and BIII-TUB (green) but not TBR1 (E, arrowhead). (G-I) Example of a RFP+ iN (red) derived from CtxAstro reprogrammed with NEUROG2 expressing GLUT (green). (J-L) Example of a RFP+ iN (red) derived from CtxAstro reprogrammed with ASCL1 expressing GABA (green). TUB: TUBULIN, GLUT: GLUTAMATE. Nuclei are stained with DAPI (blue). dpn: days post nucleofection. Scale bars: 20µm. 3 independent experiments/condition.

Figure S6. ***Related to Figure4*****. Most iNs derived from CerebAstro reprogrammed with ASCL1 express the Purkinje-cell markers CALBINDIN and CTIP2.** (A-D) Example of an RFP+ iNs derived from CerebAstro 20 dpn with ASCL1 (A, red) expressing CALB (B, green) and CTIP2 (white). Images are merged in panel D. (E) Quantification of CTIP2+ cells amongst

RFP+/CALB+ iNs. (Student t-test, Mean±SD). CALB: CALBINDIN. Nuclei are stained with DAPI (blue). Scale bars: 20µm. 3 independent experiments/condition.

Figure S7. ***Related to Figure5, 6 and 7.*** **Astroglial cells nucleofected with control plasmid, ASCL1 or NEUROG2 adopts distinct phenotypes in host postnatal cortex and olfactory bulb.** (A-C) Pictures showing GFP+ CtxAstro and CerebAstro nucleofected with control plasmid 20 dpt in postnatal cortex. Note that CtxAstro adopt a protoplasmic-like morphology in the grey matter (A), whereas cells from the same population adopt a fibrous-like morphology in the white matter (B). Note also that CerebAstro do not display morphologies reminiscent of cerebral cortex astrocytes (C). (D-I) Example of CerebAstro nucleofected with ASCL1 20 dpt in the postnatal cortex. Example of iN in layer VI of the cerebral cortex (D, dashed box), showing a GABAergic interneuron-like morphology (E). Note that iN processes are non-spiny (F, magnification of box in E). Example of GFP+ iNs found in layer I of the host cerebral cortex expressing the GABAergic interneuron marker CALB (G, dashed box). High magnification of dashed box in G showing GFP (H) and CALB (I) expression in iNs. (J) Example of GFP+ cells CtxAstro nucleofected with ASCL1 30 dpt in host postnatal cortex. Observe the cell with interneuron-like morphology (arrowhead). (K-O) Coronal sections of brains transplanted with CtxAstro nucleofected with NEUROG2 showing GFP+ axonal processes reaching (K) and within the *corpus callosum* (L-M). Note that some processes are found in the hemisphere contralateral to the transplant (N-O). (P-S) Coronal sections of the OB of animals 30 dpt of CtxAstro nucleofected with control plasmid (P, Q) or NEUROG2 (R, S) in the postnatal SVZ. Note that CtxAstro nucleofected with control plasmids migrated to OB and maintained astroglial morphology and expressed GFAP (P-Q, white arrowhead), but not NEUN (Q, red). In contrast, GFP+ cells adopted typical morphologies of granular (R) and periglomerular (S) OB neurons in

animals transplanted with CtxAstro nucleofected with NEUROG2 (R). Nuclei are stained with DAPI (blue). CALB: CALBINDIN, dpt: days post transplantation. Roman numbers in D represent the cerebral cortex layers. CC: *corpus callosum*, gcc: *genus* of the *corpus callosum*, MC: *motor cortex*, PD: *dorsal peduncular cortex.* Scale bar: 20µm. n=3-5 animals/condition.

Supplemental movies legends

Movie S1. Cerebellum astroglia nucleofected with *control-DsRed*. Frames show fluorescent images taken every 3h. Observe the glial morphology of post mitotic and proliferative cells in the culture. Last frame shows the post-imaging immunocytochemistry for DSRED (red) and BIII-TUBULIN (green). Note that all DSRED positive cells are BIII-TUBULIN negative. Label in the upper left corner indicates the time of observation in days-hours:minutes:seconds.

Movie S2. Cerebellum astroglia nucleofected with *Ascl1-DsRed*. Frames show fluorescent images taken every 3h. Observe the progressive transition in the shape of several transfected cells from a glia-like to a neuronal-like morphology. Two cells are indicated in the bottom right corner with red circles to facilitate the observation. Last frame shows the post-imaging immunocytochemistry for DSRED (red) and BIII-TUBULIN (green), where it is possible to observe the high number of DSRED+/BIII-TUBULIN+ cells. Label in the upper left corner indicates the time of observation in days-hours:minutes:seconds.

Movie S3. Cerebellum astroglia nucleofected with *Neurog2-DsRed*. Frames show fluorescent images taken every 3h. The cell tracked in the upper left corner (purple circle) undergo one circle of cell division generating two daughter cells. One cell progress to lineage-conversion into neuron and the second dies out. Note also the massive cell death of NEUROG2-transfected cells. Last frame shows the post-imaging immunocytochemistry for DSRED (red) and BIII-TUBULIN (green), where it is possible to confirm the DSRED+/BIII-TUBULIN+ cells nature of the tracked cell. Label in the upper left corner indicates the time of observation in days-hours:minutes:seconds.

Movie S4. Cerebellum astroglia nucleofected with *Neurog2-DsRed*. Frames show phase contrast images taken every 30min (same field as in MovieS3.). The cell tracked in the upper left corner (purple circle, #1) undergo one circle of cell division generating two daughter cells (white circle, #2 and red circle, #3). One cell progress to lineage-conversion into neuron (#3) and the second dies out (#2). Label in the upper left corner indicates the time of observation in days-hours:minutes:seconds.

Figure S1

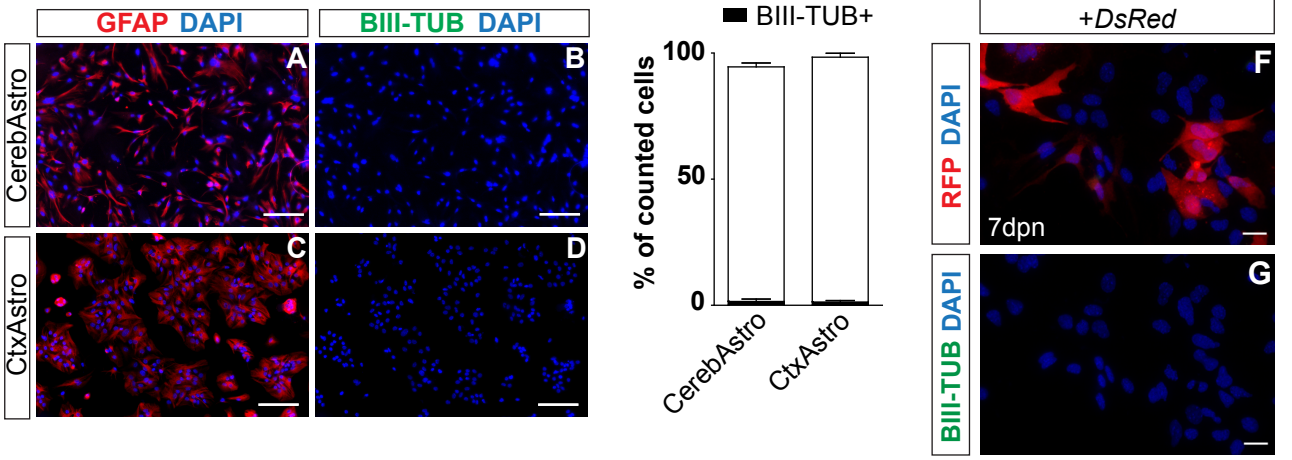

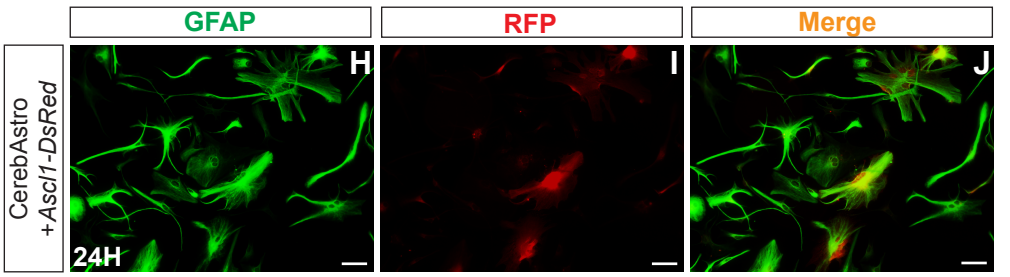

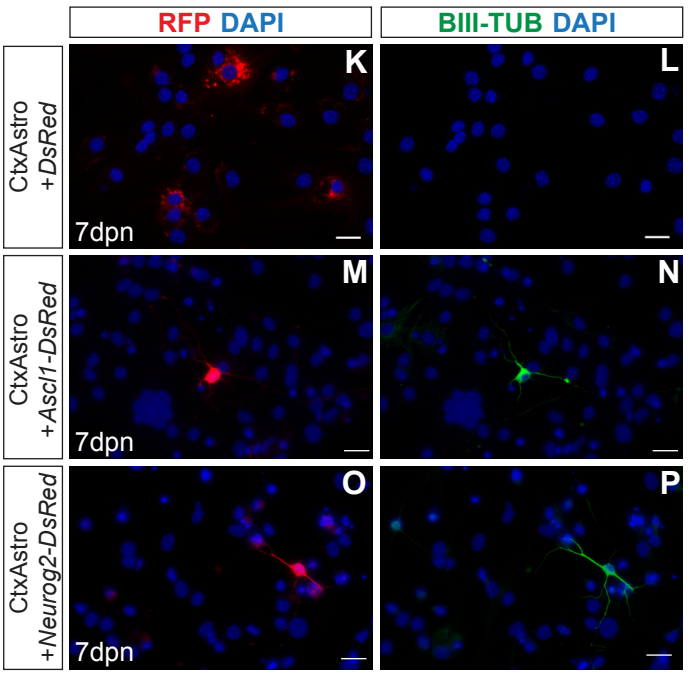

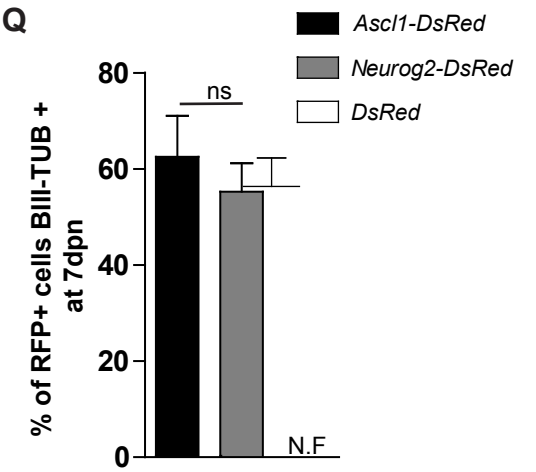

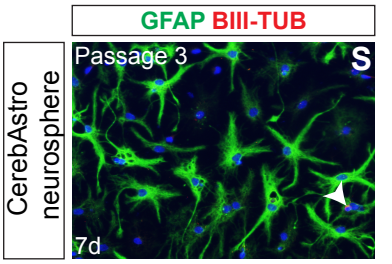

R

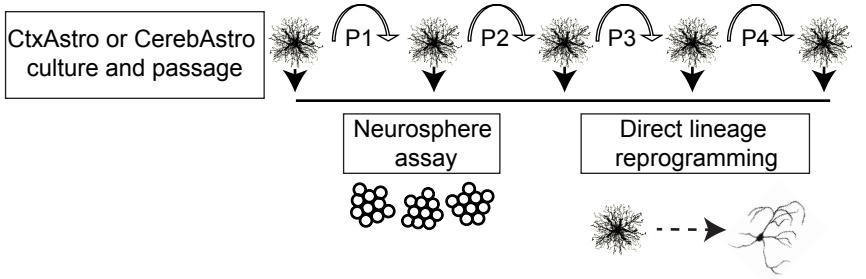

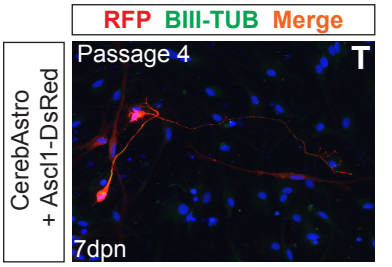

U

	Cerebral cortex astrocytes				Cerebellum astrocytes			
Passage	P1	P2	P3	P4	P1	P2	P3	P4
Neurosphere formation	++++	++	+	+	++++	+++	++	+
Mean population doubling time (h)	ND	115h	218h*	Plateau	ND	96h	125h	128h
Reprogramming	+++	+	+	ND	+++	+++	+++	++

Figure S2

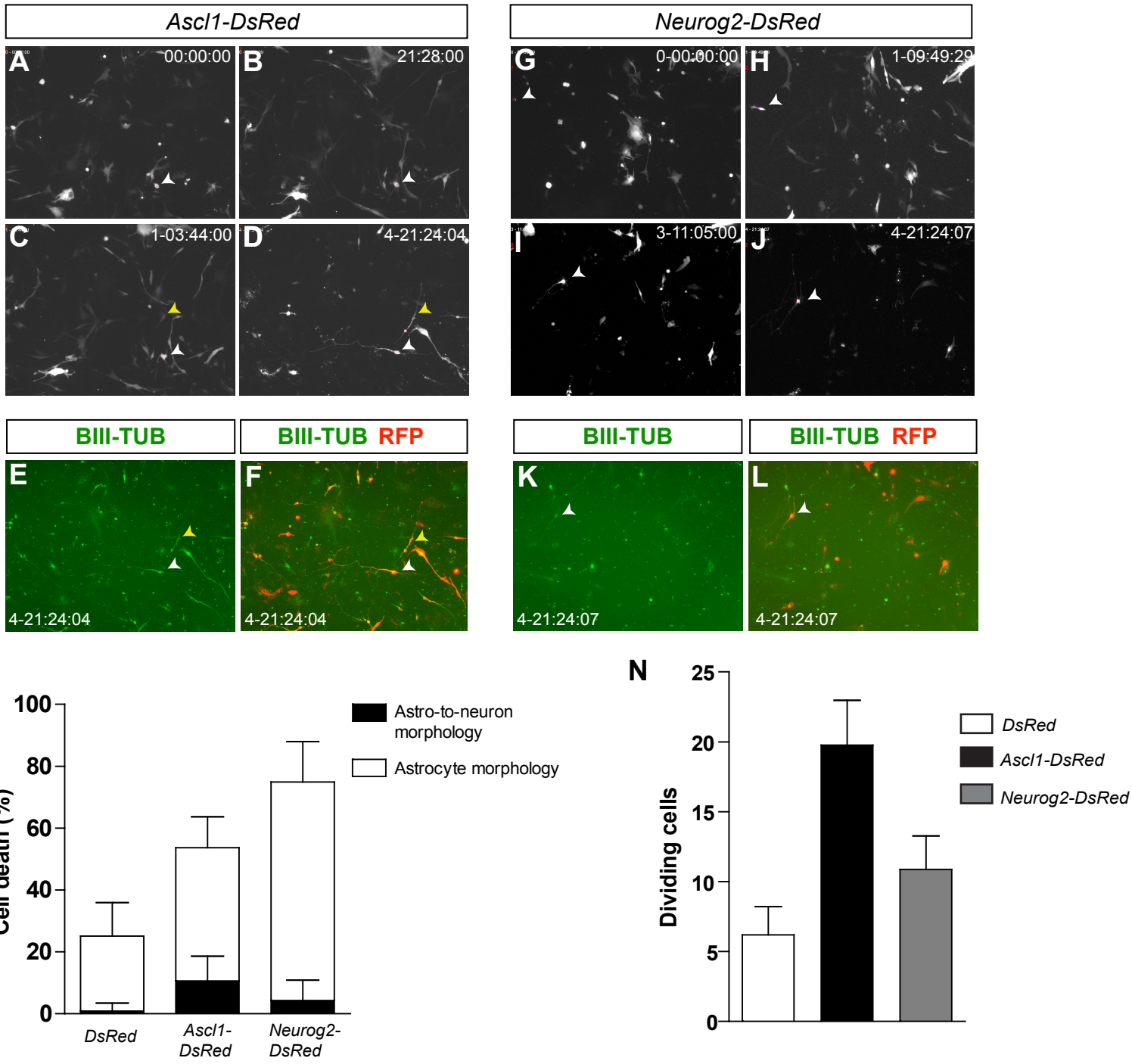
Ascl1-DsRed
Neurog2-DsRed
A
00:00:00
B
21:28:00
C
1-03:44:00
D
4-21:24:04
G
0-00:00:00
H
1-09:49:29
I
3-11:05:00
J
4-21:24:07
BIII-TUB
BIII-TUB RFP
E
4-21:24:04
F
4-21:24:04
BIII-TUB
BIII-TUB RFP
K
4-21:24:07
L
4-21:24:07

M
Cell death (%)
100
80
60
40
20
0
Astro-to-neuron morphology
Astrocyte morphology
DsRed
Ascl1-DsRed
Neurog2-DsRed

N
Dividing cells
25
20
15
10
5
0
DsRed
Ascl1-DsRed
Neurog2-DsRed

Figure S3

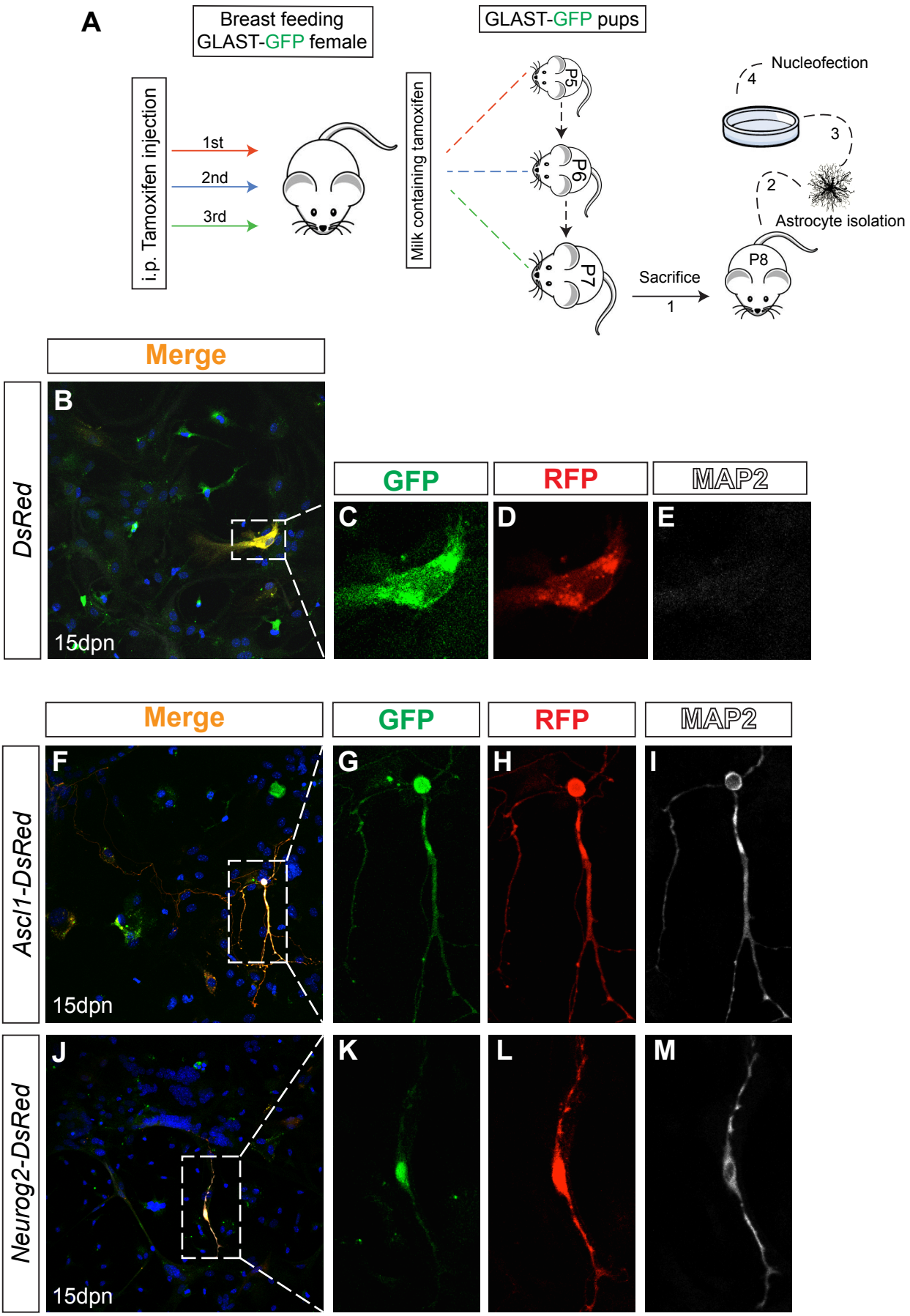
A
Breast feeding
GLAST-GFP female
GLAST-GFP pups
i.p. Tamoxifen injection
1st
2nd
3rd
Milk containing tamoxifen
P5
P6
P7
P8
Nucleofection
4
3
2
Astrocyte isolation
Sacrifice
1
Merge
DsRed
B
15dpn
GFP
RFP
MAP2
C
D
E
Merge
GFP
RFP
MAP2
Ascl1-DsRed
F
G
H
I
15dpn
Neurog2-DsRed
J
K
L
M
15dpn

Figure S4

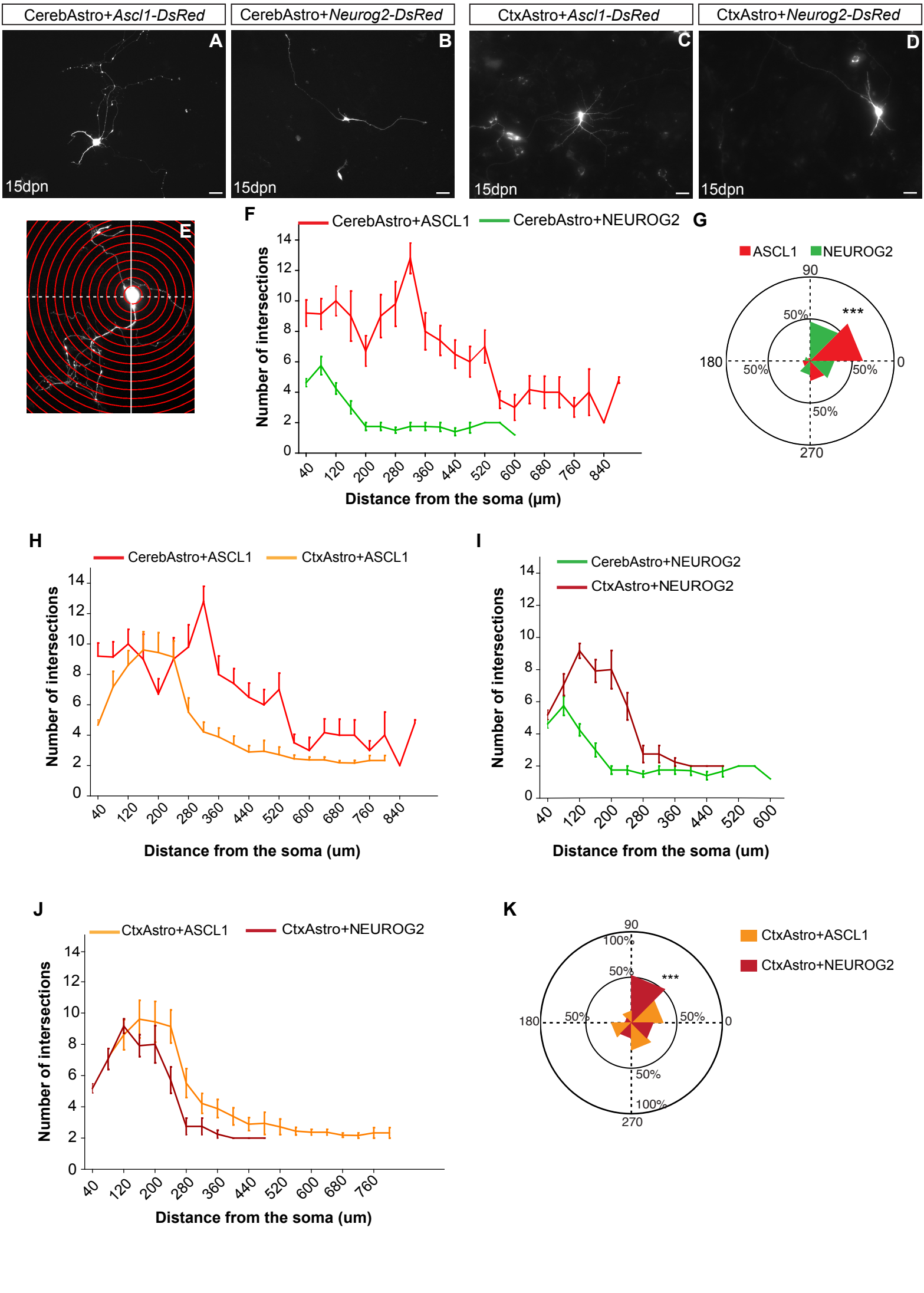
CerebAstro+Ascl1-DsRed
CerebAstro+Neurog2-DsRed
CtxAstro+Ascl1-DsRed
CtxAstro+Neurog2-DsRed
A
B
C
D
15dpn
E
F
CerebAstro+ASCL1
CerebAstro+NEUROG2
Number of intersections
Distance from the soma (μm)
G
ASCL1
NEUROG2
***
H
CerebAstro+ASCL1
CtxAstro+ASCL1
Distance from the soma (um)
I
CerebAstro+NEUROG2
CtxAstro+NEUROG2
J
CtxAstro+ASCL1
CtxAstro+NEUROG2
K

Figure S5

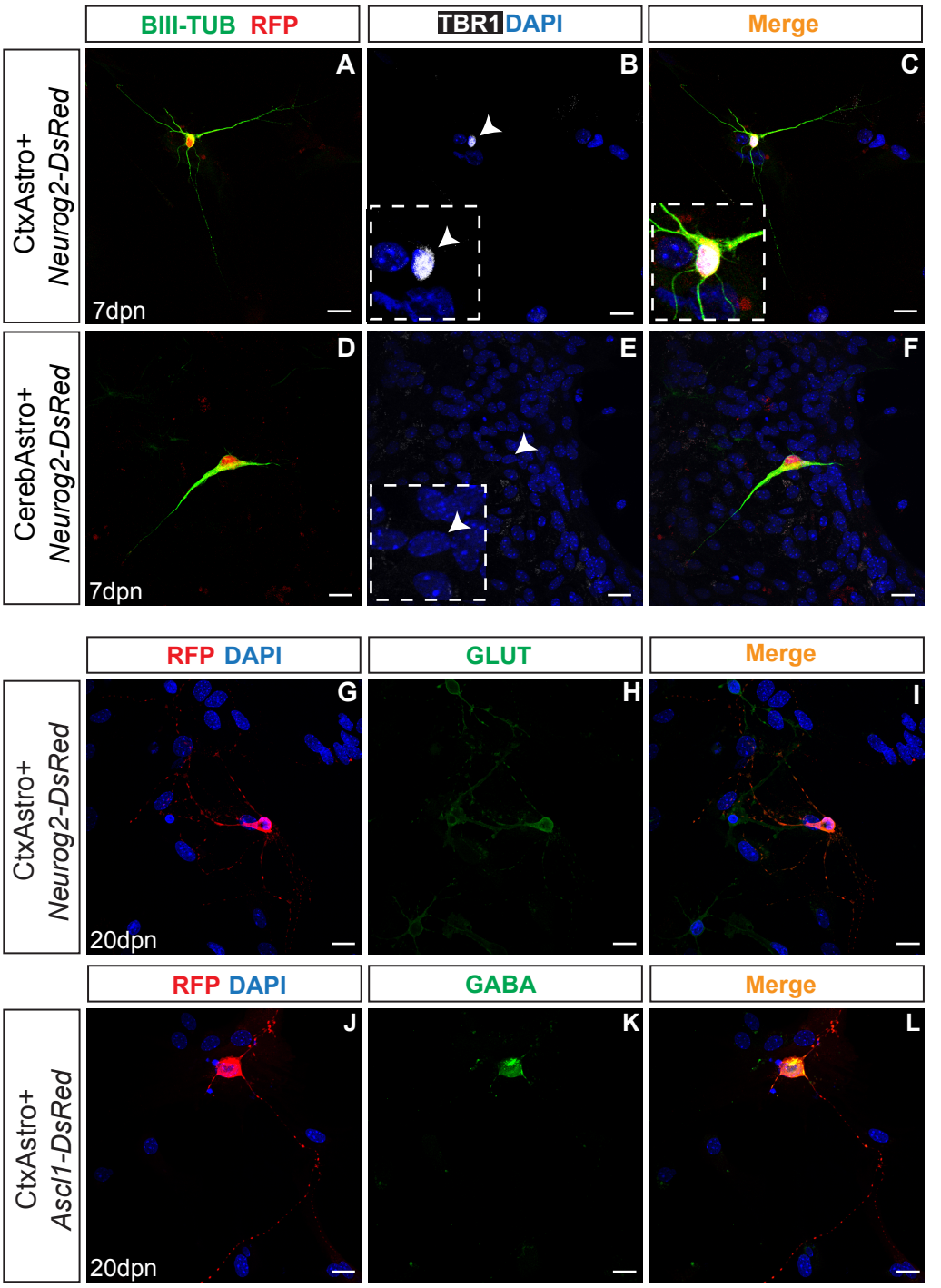
BIII-TUB RFP
TBR1 DAPI
Merge
CtxAstro+ Neurog2-DsRed
CerebAstro+ Neurog2-DsRed
CtxAstro+ Neurog2-DsRed
CtxAstro+ Ascl1-DsRed
RFP DAPI
GLUT
GABA
A
B
C
D
E
F
G
H
I
J
K
L
7dpn
20dpn

Figure S6

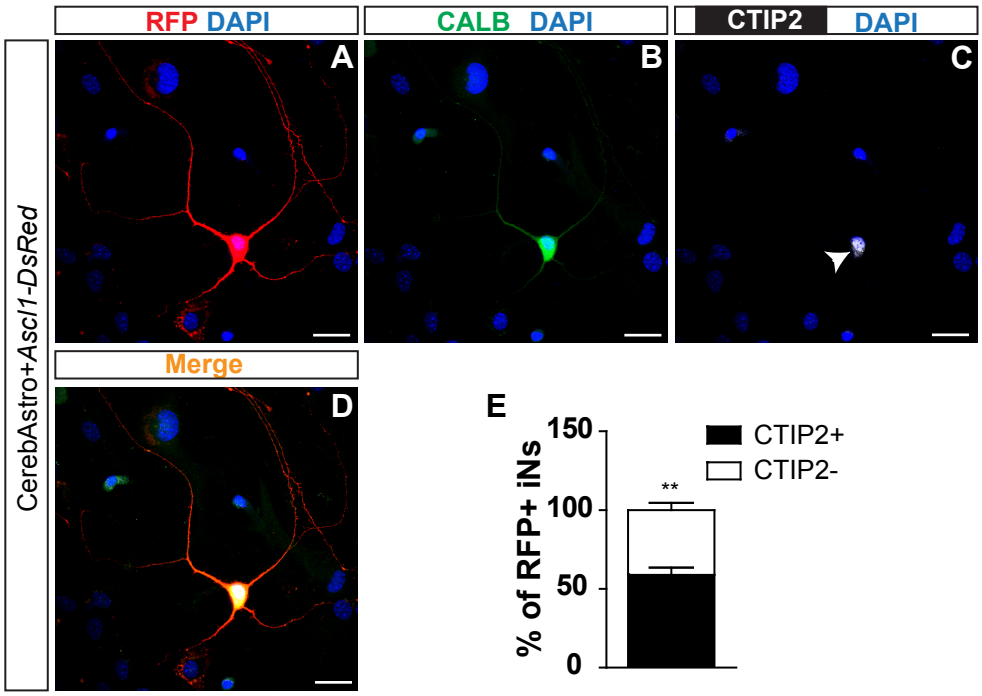
RFP DAPI
CALB DAPI
CTIP2 DAPI
A
B
C
CerebAstro+Ascl1-DsRed
Merge
D
E
150
100
50
0
% of RFP+ iNs
CTIP2+
CTIP2-
**

Figure S7

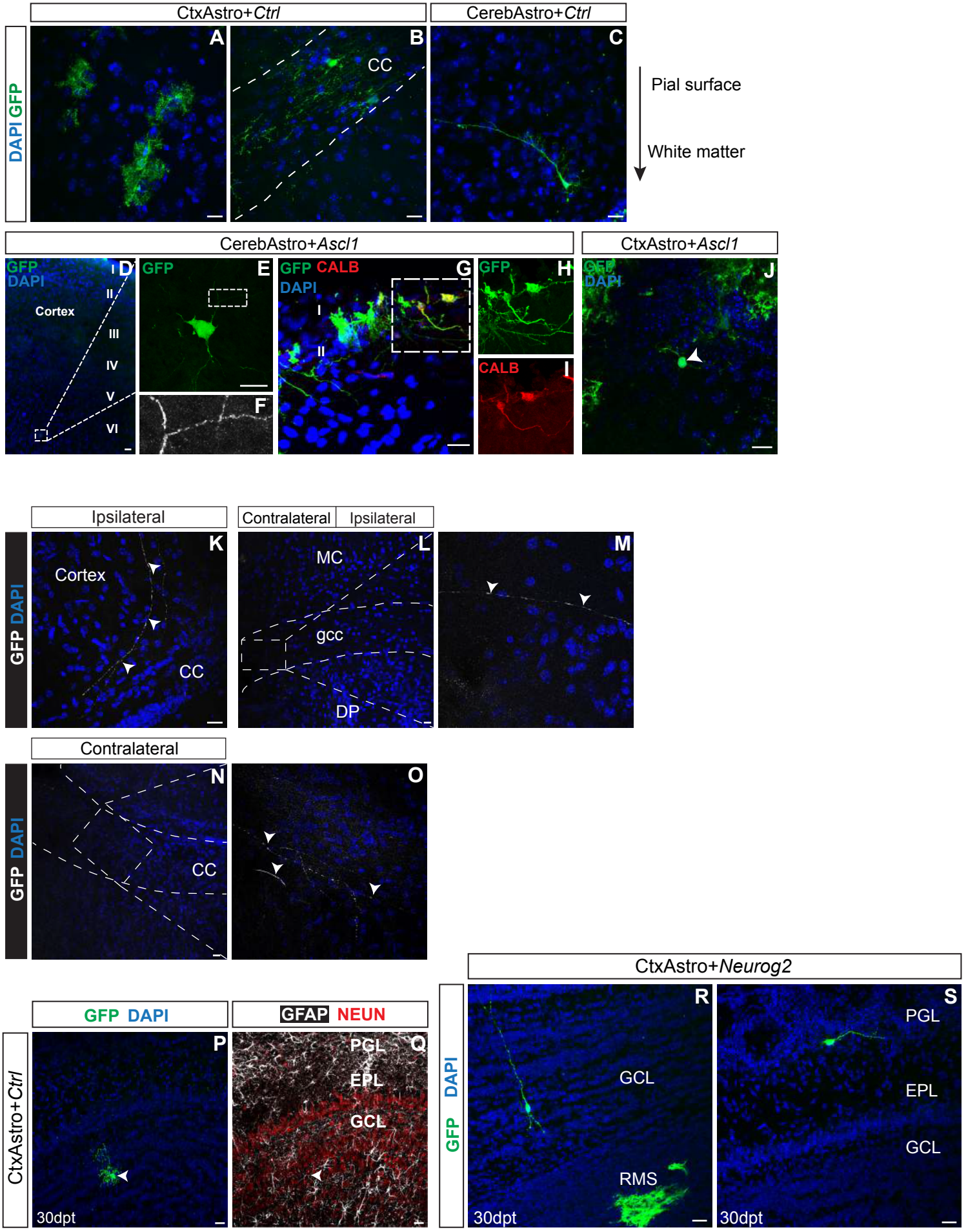
CtxAstro+Ctrl
CerebAstro+Ctrl
DAPI GFP
A
B
CC
C
Pial surface
White matter
CerebAstro+Ascl1
CtxAstro+Ascl1
GFP DAPI
D
Cortex
II
III
IV
V
VI
GFP
E
F
GFP CALB DAPI
G
I
II
GFP
H
CALB
I
GFP DAPI
J
Ipsilateral
Contralateral
Ipsilateral
GFP DAPI
K
Cortex
CC
L
MC
gcc
DP
M
Contralateral
GFP DAPI
N
CC
O
CtxAstro+Neurog2
GFP DAPI
GFP DAPI
GFAP NEUN
CtxAstro+Ctrl
P
30dpt
PGL
Q
EPL
GCL
R
GCL
RMS
30dpt
S
PGL
EPL
GCL
30dpt